Sustainable Cities and Society 103 (2024) 105262

Contents lists available at ScienceDirect

Sustainable Cities and Society

journal homepage: www.elsevier.com/locate/scs

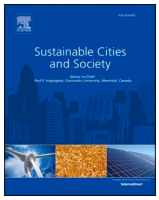

Accessing eye-level greenness visibility from open-source street view images: A methodological development and implementation in multi-city and multi-country contexts

Ilse Abril Vázquez Sánchez, S.M. Labib *

Department of Human Geography and Spatial Planning, Faculty of Geosciences, Utrecht University, Utrecht 3584 CB, the Netherlands

ARTICLE INFO

Keywords:
Green View Index
Image segmentation
Google Street View
Normalised Difference Vegetation Index
Greenspace
Green Infrastructure

ABSTRACT

The urban natural environment provides numerous benefits, including augmenting the aesthetic appeal of urban landscapes and improving mental well-being. While diverse methods have been used to evaluate urban greenery, the assessment of eye-level greenness visibility using street-view level images is emerging due to its greater compatibility with human perception. Many existing studies predominantly rely on proprietary street view images provider such as Google Street View (GSV) data; the usage restrictions and lack of alignment with FAIR (**F**indability, **A**ccessibility, **I**nteroperability, and **R**eusability) principles present challenges in using proprietary images at scale. Therefore, incorporating Volunteered Street View Imagery (VSVI) platforms, such as Mapillary, is emerging as a promising alternative. In this study, we present a scalable and reproducible methodological framework for utilising Mapillary images for Green View Index (GVI) assessment using image segmentation approach and evaluate the completeness and usefulness of such data in diverse geographical contexts, including eleven cities (i.e., Amsterdam, Barcelona, Buenos Aires, City of Melbourne, Dhaka, Ho Chi Minh, Kampala, Kobe, Mexico City, Seattle, and Tel Aviv). We also evaluate the use of globally available satellite-based vegetation indices (e.g., Normalised Difference Vegetation Index-NDVI) to estimate GVI in locations where street-view images are unavailable. Our approach demonstrates the applicability of Mapillary data for GVI assessments, although revelling considerable disparities in image availability and usability between cities located in developed and developing countries. We also identified that the NDVI could be used effectively to estimate GVI values in locations where direct street-level imagery is limited. Additionally, the analysis reveals notable differences in greenness visibility across cities, particularly in high-density, lower-income cities in Africa and South Asia, compared to low-density, high-income cities in the USA and Europe.

1. Introduction

Greenspaces play a crucial role in urban environments, offering a wide array of social, environmental, and ecological benefits (Bain et al., 2012; Gómez-Baggethun & Barton, 2013; Barona et al., 2023; Saw et al., 2015). As the urban population is projected to increase by 60 % by 2050 (United Nations, Department of Economic, & Social Affairs, 2019), sustainable development becomes imperative in addressing pressing issues, including climate change mitigation and improving the quality of life for urban residents (Nieuwenhuijsen, 2020; Labib et al., 2020a). Urban green spaces provide multifunctionality to enhance the environmental quality within cities. They effectively mitigate the heat island effect (Keeley, 2011; Lafortezza et al., 2009), improve air quality by reducing pollutants (Akbari et al., 2001; Jim & Chen, 2008), reduce noise pollution (Attal et al., 2021; Wong et al., 2010), and minimise stormwater runoff (Armson et al., 2013; Berland et al., 2017). Moreover, the visual perception of street greenery is recognised as a vital sensory function that positively influences individuals' experiences in urban settings (Lu et al., 2018; Wolf, 2005). Urban greenery serves as a protective barrier against visual intrusion (Li et al., 2015a). Furthermore, the presence of vegetation in urban landscapes often leads to higher aesthetic perception of streetscapes (Lindemann-Matthies & Brieger, 2016), promoting physical activities (Zijlema et al., 2020) and fostering social cohesion among residents (Root et al., 2017). From a health perspective, visual contact with greenery also evokes positive emotions, reduces stress, and facilitates the recovery of mental fatigue (Kaplan,

* Corresponding author.
E-mail addresses: s.m.labib@uu.nl, labib.l.m@gmail.com (S.M. Labib).

https://doi.org/10.1016/j.scs.2024.105262
Received 3 July 2023; Received in revised form 14 December 2023; Accepted 7 February 2024
Available online 8 February 2024

1995; Ulrich, 1984; Wang et al., 2022).

Different assessment methods have been employed to measure and evaluate urban greenery, including surveys, interviews, and audits, to gain insights into people's opinions and attitudes toward street-level views of urban greenery (Falfán et al., 2018; Li et al., 2015b). However, each of these methods has its advantages and limitations. Surveys using questionnaires may be more reflective of people's personal experience on the ground but may be affected by response bias (Downs & Stea, 1977). Additionally, audits require skilled evaluators and specific criteria to assess visual aesthetic quality (Ellaway et al., 2005; Tang & Long, 2019). Such approaches may involve physically transporting evaluators to real locations for direct evaluation of environmental attributes, which can be time-consuming, expensive, and subjective to each participant (Gupta et al., 2012; Meitner, 2004; Yao et al., 2012). In contrast to interview approaches, recent advances in computational advances (e.g., Deep learning image analysis) along with high-resolution data from multiple sources such as geospatial data and street view image data allowed computational modelling of eye-level greenery at scales.

One example is the geospatial viewshed model using high-resolution light detection and ranging (LiDAR) based data, which has been extensively employed to map and quantify vegetation cover in urban areas, benefiting from their advantages in terms of repeatability, synoptic view, and wide area coverage (Li et al., 2015b). These methods involve three-dimensional data sets derived from high-resolution remotely sensed images and LiDAR, enabling the detection of tree species and the vertical dimensions of urban trees (Alonzo et al., 2014; Edson & Wing, 2011; Shrestha & Wynne, 2012). According to Yu et al. (2016), these approaches offer several advantages, such as the capacity to adjust the relative height of the observer to simulate different vertical horizons and the potential to model artificial buildings to simulate future landscapes. Nevertheless, the results depend on the original resolution and accuracy of the utilised datasets (Labib et al., 2021), and there is a risk of information loss when compressing point cloud data into a two-dimensional raster surface (Yang et al., 2020). Additionally, high-resolution LiDAR data and digital elevation raster surfaces are mostly unavailable in most cities or countries worldwide, making it difficult to use such models in diverse geographic contexts (Labib et al., 2021; 2020b).

In contrast to the viewshed-based approach, Li et al. (2015) made significant advances in this field by utilising automatically extracted Google Street View (GSV) images and employing image segmentation techniques for automating the greenery calculation process. This breakthrough has led to the emergence of several innovative computational approaches that have demonstrated a high level of agreement with human perception (Aikoh et al., 2023; Suppakittpaisarn et al., 2022; Torkko et al., 2023), offering several benefits such as reduced research time and workloads, increased accessibility, and the ability to study urban greenery without the need for physical visits to field sites (Lu et al., 2023; Rangel et al., 2022; Seiferling et al., 2017).

Another widely adopted approach is computational image segmentation, which is categorised into colour-segmentation and semantic-segmentation. Colour-segmentation method classifies images according to colour values of individual pixels, effectively identifying and delineating areas with green vegetation (Chen et al., 2020; Dong et al., 2018; Larkin & Hystad, 2019; Long & Liu, 2017). On the other hand, semantic-segmentation is a machine learning-based approach that leverages contextual information to understand and segment images (Xia et al., 2021). By assigning semantic levels to individual pixels, this method allows to comprehend the image content, facilitating precise identification and mapping of green vegetation (Cai et al., 2018; Helbich et al., 2019; Ki & Lee, 2021; Kido et al., 2021; Xia et al., 2021; Ye et al., 2019. Recently, Torkko et al. (2023) investigated different eye-level greenery extraction methods and found the image segmentation approach aligns better with human perception than colour-based segmentation. The colour-based segmentation approach is sensitive to lighting conditions (Batlle et al., 2000; Pietikainen et al., 1996), and they also tend to misclassify green paint as greenery, leading to overestimating green areas (Larkin & Hystad, 2019; Li et al., 2015b).

Numerous recent studies employing image segmentation for vegetation analysis heavily rely on data from GSV (Cai et al., 2018; Chen & Biljecki, 2023; Jimenez et al., 2022; Rzotkiewicz et al., 2018). However, it is crucial to acknowledge the barriers and limitations surrounding data access and usage (Inoue et al., 2022; Zheng & Amemiya, 2023). In particular, GSV imposes restrictions on the use of imagery, including limitations on data analysis and extraction (Google, 2018b, 2020). As stated by Rundle et al. (2022), the restriction on certain uses of Google Maps is not grounded in copyright law, which would potentially allow researchers to invoke the "Fair" use principles. Rather, these limitations are based on the contractual agreement that users must adhere to when accessing Google Maps (Google, 2018a). The enforceability of such contracts is currently subject to ongoing legal disputes, making it uncertain. Consequently, researchers engaging in this type of research and the journals publishing the resulting papers assume some legal risk as long as the legal status remains unsettled (Rundle et al., 2022; Stringam et al., 2023). In addition, using such data might hinder the adoption of FAIR (**F**indable, **A**ccessible, **I**nteroperable, and **R**eusable) data principles in scientific research (Wilkinson et al., 2016). GSV is often easy to find, usually has more extensive geographic coverage than other street view image sources, and is interoperable with other data (e.g., mostly provided by Google). Additionally, GSV uses more consistent image capture methods and instruments, thus usually maintaining high consistency and image quality. However, they are not widely accessible due to restrictions on the number of free downloads; there is a limit to the quantity of data that can be obtained without incurring charges (Zheng & Amemiya, 2023; Google, 2023). This means that researchers who require a considerable amount of GSV data may encounter financial barriers. This inaccessibility also results in a lack of reusability of such data by others. These attributes do not align with the open-access data characteristics, which need to be freely accessible without any restriction for everyone. Considering these aspects, it can be argued that although GSV has some characteristics that match a few aspects of FAIR principles, the whole GSV data does not meet the FAIR and open-access data principles.

To overcome GSV limitations, integrating Volunteered Street View Imagery (VSVI) platforms, such as Mapillary and Open Street Cam, has been developed over the years (Alvarez Leon & Quinn, 2019; Yu et al., 2019; Zheng & Amemiya, 2023). Mapillary, in particular, stands out as the largest crowdsourcing-based street view platform, boasting a community of over 20,000 users who contribute street-level photos using GPS-enabled cameras or smartphones (Ma et al., 2020). Notably, Mapillary adopts an open data approach by realising imagery under the Creative Commons Attribution-ShareAlike 4.0 International license (Alvarez Leon & Quinn, 2019). This open data policy enables researchers to utilise the imagery more freely, including for commercial purposes, fostering innovation and collaboration in studying urban greenery and related phenomena (Alvarez Leon & Quinn, 2019).

While Mapillary provides an alternative solution through its open data approach, researchers are aware of its limitations, as these can affect the reliability and accuracy of the data (Antequera et al., 2020; D'Andrimont et al., 2018; Juhász & Hochmair, 2016; Krylov & Dahyot, 2019). Firstly, the quality of the imagery contributed by users on Mapillary may vary significantly due to differences in camera properties, including various camera models (with varying sensors) and settings (e.g., focal length) used by contributors (Antequera et al., 2020). These variations can result in differences in resolution, blurring, restricted field of view, and reduced visibility (D'Andrimont et al., 2018). Secondly, Mapillary primarily relies on forward-facing cameras mounted on vehicles driven on roads, resulting in linear motion without rotation, limiting the perspectives captured in the imagery and potentially limiting the comprehensive understanding of the surroundings (Antequera et al., 2020; Krylov & Dahyot, 2019). Finally, the level of engagement and participation from users can vary across different regions and communities, leading to disparities in data availability, in

particular cities in developing countries often have low volunteer engagement in data collection (D'Andrimont et al., 2018; Nielsen, 2006). As a result, researchers relying solely on Mapillary may encounter gaps in the coverage of specific locations or road segments that can limit the ability to obtain a complete and representative sample of the desired study area (Juhász & Hochmair, 2016).

In contrast to missing street view image in certain locations, satellite-derived top-down measures of greenery, such as the Normalised Difference Vegetation Index (NDVI), is globally available at any place and often widely used in measuring greenness modelling (Martinez & Labib, 2023). It can be argued that for situations where there is insufficient street image data to determine the GVI, an alternative approach is to utilise NDVI to estimate GVI using statistical models. Although NDVI is a top-down measure and may not capture the actual visibility of greenery (Labib et al., 2021), as NDVI represents available vegetation, it can be assumed that a model can learn from the relation between known GVI and NDVI within a certain distance zone to impute GVI for unknown locations. In this regard, Torkko et al. (2023) indicated that mean NDVI values within smaller distances (e.g., 50 m) from observation points might represent perceived visible greenery. In a different research, O'Regan et al. (2022) demonstrated a methodology to estimate air pollution, incorporating GVI, NDVI, and other variables. Thus, using NDVI to estimate GVI can be a potential solution to fill the street view data gaps for modelling greenness visibility.

A few studies have demonstrated the potential of utilising Mapillary's images for evaluating and quantifying urban greenness visibility (Liang et al., 2022; Yap et al., 2022), and numerous studies have used NDVI to measure the presence of greenery (Martinez & Labib, 2023). Despite these promising findings regarding the potential use of the data source, there remains an absence of systematic evaluation regarding the usability of Mapillary data in different urban contexts for estimating greenness visibility and the potential of using NDVI to estimate greenness visibility in missing locations. Additionally, there is a lack of complete methodological workflow to use Mapillary data in different places and reproduce these analyses, hindering the usage of such open-source and FAIR data in modelling greenness visibility in diverse geographic contexts.

To address the methodological limitations and exiting research gaps noted above, this study aims to provide a scalable, reproducible methodological framework for utilising Mapillary data for greenness visibility modelling as well as evaluate the completeness and usefulness of such data in diverse geographical contexts. The primary objective is to establish a robust and replicable methodology that can be applied for greenness visibility modelling at any location. Additionally, the secondary objective of this study is to evaluate the use of NDVI to estimate GVI in locations where street-view images are unavailable. To achieve these objectives, this study will examine the following research questions:

RQ(1) How does the image availability and usability of Mapillary data for green view assessments varies across different cities worldwide?
RQ(2) To what extent is the NDVI suitable for filling in missing data points in the GVI assessment?
RQ(3) Are there differences in street-level greenness visibility between cities located in different geographic contexts?

To answer these questions, we will conduct a comparative analysis of the GVI across different cities worldwide, allowing to assess the quality and completeness of the data available through Mapillary. This comparative approach will provide insights into the reliability and applicability of the platform for greenness visibility assessments in different parts of the world. The development of this methodology aims to democratise the analysis of urban greenness, making it FAIR for researchers, urban planners, and policymakers interested in assessing and monitoring the visibility of greenery in their cities. By establishing such a methodology, our project seeks to foster a better understanding of the relationship between urban natural environments, human well-being, and urban sustainability.

2. Methodology

2.1. Study areas

Our study examines a diverse range of cities across diverse geographic, demographic, and socioeconomic contexts and located in multiple countries and continents. The cities included in our research are Amsterdam, Netherlands; Barcelona, Spain; Buenos Aires, Argentina; City of Melbourne, Australia; Dhaka, Bangladesh; Ho Chi Minh, Vietnam; Kampala, Uganda; Kobe, Japan; Mexico City, Mexico; Seattle, USA; and Tel Aviv, Israel. Amsterdam, Barcelona, City of Melbourne, Kobe, Seattle, and Tel Aviv are known for their advanced urban planning and commitment to environmental sustainability initiatives (Bush et al., 2021; Dierwechter, 2017; Herscovici et al., 2022; Mora & Bolici, 2017). These cities, situated in developed nations, have been able to invest significantly in their infrastructure, incorporating technology and innovation to enhance their urban environments (Bush et al., 2021; Dierwechter, 2017; Herscovici et al., 2022; Mora & Bolici, 2017). In contrast, Buenos Aires, Ho Chi Minh, Dhaka, Kampala, and Mexico City, located in developing regions, face unique challenges related to rapid urbanization (Abebe, 2013; Aguilar & Lopez, 2018; Mortoja & Yigitcanlar, 2022). These cities experience high population growth and often face issues of limited resources in terms of infrastructure and public services (Abebe, 2013; Aguilar & Lopez, 2018; Mortoja & Yigitcanlar, 2022; Labib et al., 2020a). Their inclusion in the study provides a contrasting perspective on urban development and the role of Volunteered Street View Imagery (VSVI), such as Mapillary, in dynamic and resource-constrained contexts. Since one of our aims is to evaluate the quality and completeness of the data available through Mapillary, we assume that these diverse cities will provide valuable insights into the reliability and applicability of the platform for assessing greenness visibility in different parts of the world using open-source images. It will also allow identifying variations or limitations in the data between cities.

2.2. Data sources

The data sources for this study primarily consisted of open-source platforms, which provided access to a wide range of geospatial data. Three major data sets were utilised in this research, namely: the Street Network with OSMnx, the VSVI with Mapillary, and the Satellite-Derived NDVI.

2.2.1. Street network with OSMnx

Street network data was retrieved using OSMnx, an open-source Python library specifically developed for working with Open Street Map (Boeing, 2017). OSMnx provides a convenient set of functions and methods for downloading and processing street network graphs for specific regions. Our research employed this library to extract simplified street network data, with a specific focus on obtaining street link information.

2.2.2. VSVI with Mapillary

The VSVI data was obtained by using the Mapillary API (Mapillary, 2021). We selected Mapillary as it is the largest VSVI source, with more than one billion nine hundred million images available globally. According to Ma et al. (2020), as of February 2019, Mapillary had a substantial user base of 21,948 contributors worldwide, with a considerable concentration in Europe and North America. These regions have abundant street view imagery, particularly in the United States, Germany, Sweden, and Italy, as a few major users continually contributed to collecting a large share of images. In contrast, data remains notably sparse

across several Asian and African countries (Ma et al., 2020; Juhász & Hochmair, 2016). The number of consistent contributors has steadily grown by more than 100 annually, ensuring the project's continued healthy evolution, but it is expected that disparities in image coverage will remain. In particular cities in developing countries, Maplliary data quality and unavailability are continuing challenges. Despite such limitations, this is the largest VSVI data source that follows FAIR data principles; therefore, we considered Maplliary in this study. Further details on the overall evaluation of Mapillary data completeness and user contribution can be found in Ma et al. (2020).

The API provides access to vector tiles endpoints that contain information such as the position of images and sequences with their original geometries. Within the coverage tiles endpoint, three layers are available: overview, sequence, and image. For our research, we focused on the image layer, which contains details such as the compass angle of the image, the timestamp of image capture, the image ID, and a flag indicating whether it is a panoramic image.

2.2.3. Satellite-derived Normalised Difference Vegetation Index

The Satellite-Derived NDVI data were used in our study to determine the GVI on points in areas where images were unavailable. Specifically, the NDVI data was derived from Sentinel-2 satellite imagery, which offers a resolution of 10 m (Satellite Imaging Corporation, 2022) and often performs better in detecting urban vegetation than other satellite images such as Landsat and MODIS (Labib & Harris, 2018; Markevych et al., 2017). Certain criteria were applied in selecting satellite imagery to ensure the quality and reliability of the NDVI data. Firstly, the chosen imagery had a cloud cover of less than 10 % to mitigate the potential distortion caused by clouds, which can obstruct the accurate assessment of vegetation indices (Meraner et al., 2020). Secondly, the selected satellite imagery was collected considering the best pixel over the course of the year 2020. This approach involved selecting the image with the most favourable conditions for vegetation analysis within the given time frame, maximising the accuracy and representativeness of the NDVI data for the analysis (Corbane et al., 2020). We used estimate NDVI Google Earth Engine (GEE) to identify images within the period spanning the first and last day of 2020, from which a composite image was generated.

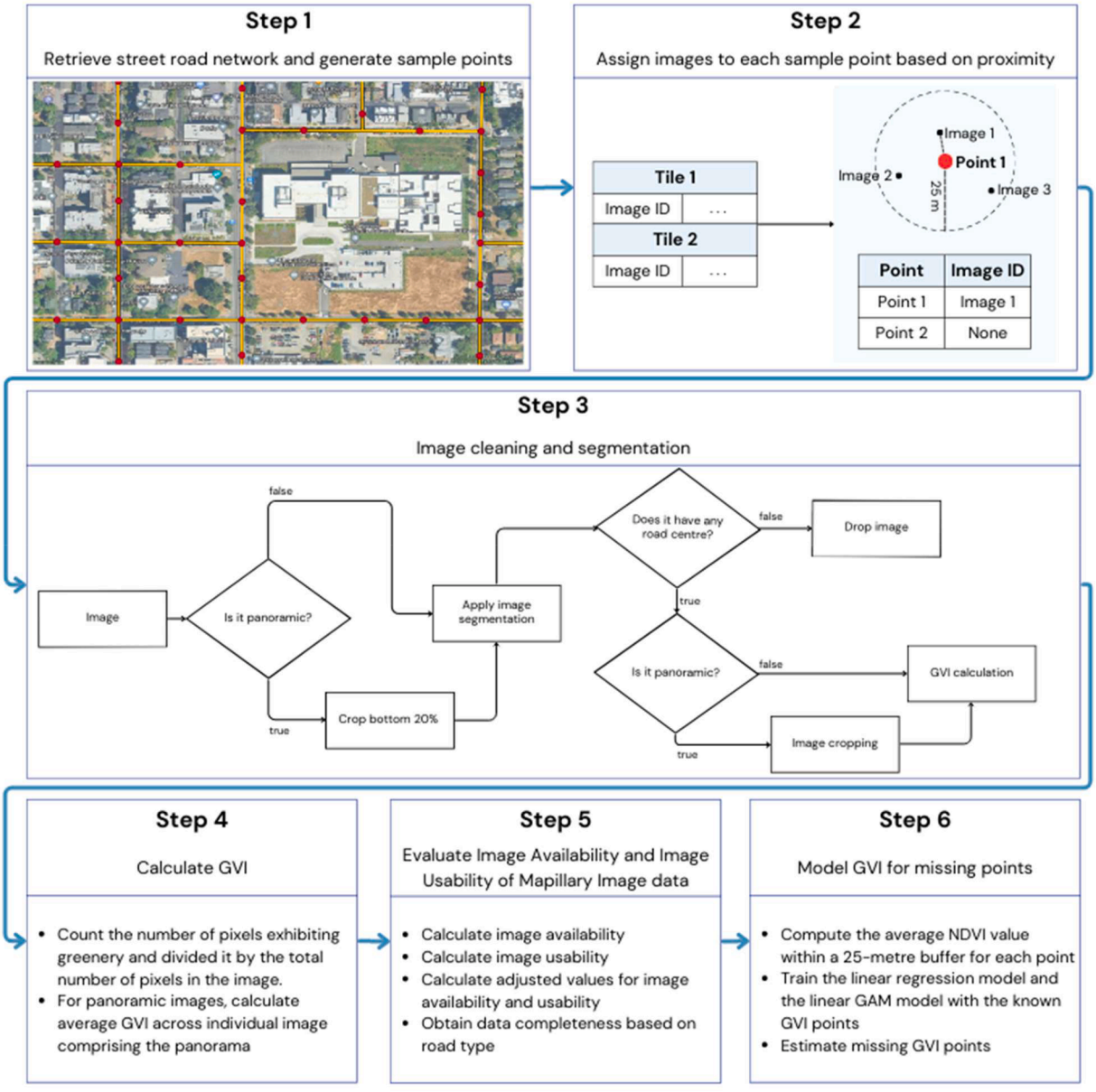

Fig. 1. Methodology overview, which is openly accessible in GitHub: https://github.com/Spatial-Data-Science-and-GEO-AI-Lab/StreetView-NatureVisibility.

The composite image consisted of pixels with the median value across all identified pixels based on the criteria noted above. The NDVI values range from -1 to +1, where a value of -1 represents water, values around 0.2 suggest vegetation coverage, and higher values indicate denser forest coverage (Martinez & Labib, 2023). To ensure that only image pixels potentially containing vegetation were considered, values below 0 were removed from the analysis.

2.3. Modelling GVI using open source data

2.3.1. Step 1. Retrieve street road network and generate sample points

Fig. 1 shows an overview of our methodology. First, the simplified street network data, represented as a graph object with nodes and edges, was obtained from OSMnx by indicating the name of the city to be analysed (e.g., "Amsterdam, Netherlands"). It is worth noting that bidirectional streets are represented as two separate overlapping roads, with the starting and ending nodes inverted. To avoid analysing the same road twice, we implemented a filtering strategy to retain only one of the duplicate roads and geographically projected the cleaned network. Once the street network data was cleaned, we proceeded to conduct point sampling at regular intervals of 50 m along the roads. These sampled points serve as reference locations for selecting the corresponding images from Mapillary, which were then used to analyse the GVI. It should be noted that the sampling intervals determine the number of locations sampled, which might impact the estimated distribution of GVI values based on the number of sample locations that have been generated in each study area, which can vary depending on the size of the city. However, as it is computationally challenging to sample at every 1 or 5 m, we selected 50 m as a reasonable sample interval to extract images. Our selection of 50 m intervals aligns with several previous studies which analysed GVI at 50–100 m sampling distances along the streets (Ki & Lee, 2021; Wang et al., 2021; Chen et al., 2019; Helbich et al., 2019).

2.3.2. Step 2. Assign images to each sample point based on proximity

To access the VSVI data, requests need to be made to the Mapillary API using the tile coordinates and zoom level of 14 (Mapbox, 2023). Therefore, to implement the data retrieval, we divided the area covered by the obtained road network into tiles. For each tile, we accessed the metadata of all the available images within it. Subsequently, we assigned one image to each sample point in the road network based on their proximity using the cKDTree algorithm (SciPy, 2022). In our case, the algorithm was queried to identify the closest neighbour within a maximum distance of 25 m from each sample point. This distance was chosen based on the spacing of the sample points, which are 50 m apart. By using this distance, we can ensure that no two points will be assigned the same image. Once we had determined the image ID of the closest image to each sample point, we were able to access the corresponding image by using the URL provided by the image endpoint (Mapillary, 2021).

2.3.3. Step 3. Image cleaning and segmentation

After obtaining the image, the subsequent step involved semantic image segmentation and image filtering process to clean and segment the images for further processing. To begin, for panoramic images, we performed a cropping operation, illustrated in Fig. 2, to remove the bottom 20 % of the image (Fig. 2a, b). This area corresponds to a band captured by the camera that is present in all panoramic images. By removing this band, we ensured that only the relevant portions of the image were retained for further analysis.

In the next stage, we applied the Masked-attention Mask Transformer (Mask2Former) architecture-based image segmentation model (Cheng et al., 2022) to segment the images into different objects. The Mask2-Former (Fig. 3) is a powerful architecture designed for universal image segmentation, encompassing tasks such as panoptic segmentation, instance segmentation, and semantic segmentation (Cheng et al., 2022).

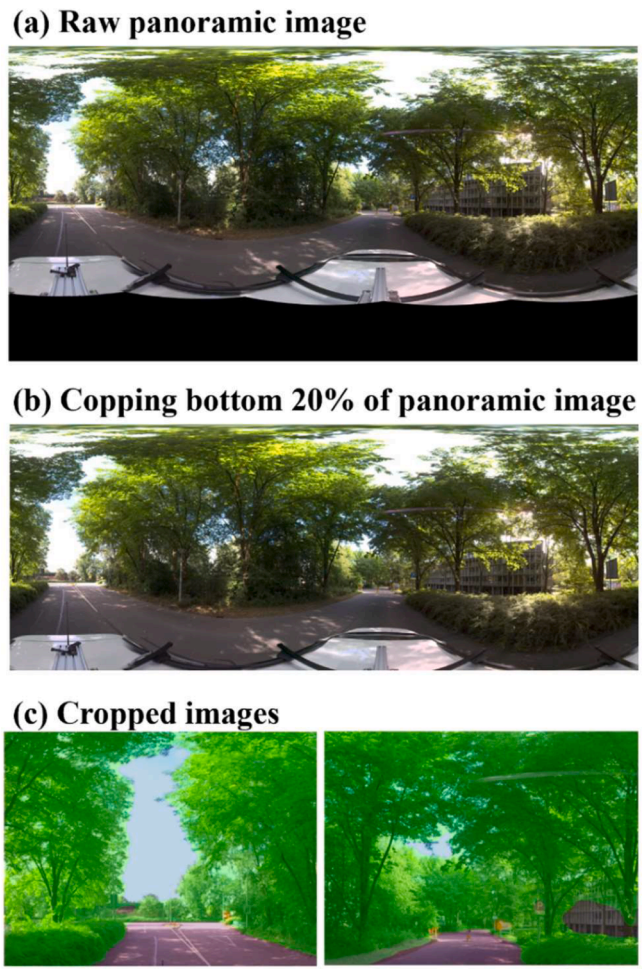

Fig. 2. Processing images, (a) raw panoramic image without any cropping, (b) cropping the bottom part of the image, (c) copped images from panorama.

The Mask2Former model incorporates several key components to achieve its capabilities. One of the central elements is the use of masked attention, a mechanism that enables the extraction of localised features by constraining cross-attention within predicted mask regions. By doing so, the model can focus on relevant regions and capture fine-grained details, resulting in highly accurate segmentation results (Cheng et al., 2022).

The performance of Mask2Former was evaluated on four popular datasets: Common Objects in Context (COCO), Cityscapes, ADE20K, and Mapillary Vistas (Cheng et al., 2022). Notably, when tested on the Mapillary Vistas dataset, the model achieved impressive mean intersection over union (mIoU) scores of 57.4 for small objects and 59.0 for medium and large objects. These results underscore the competitive performance of Mask2Former compared to other state of-the-art methods on Mapillary Vistas (Cheng et al., 2022). In our study, Mask2Former enabled the identification and classification of different objects within the images, including vegetation and roads, that were used for subsequent analysis.

To determine the suitability of each image for analysis, we employed an algorithm designed to identify the road centres from the segmented image (Fig. 2c). If road centres were detected, then the image was considered suitable and retained for further calculation (Fig. 4a, b). Conversely, if no road centres were identified, the image was deemed unsuitable and subsequently discarded (Fig. 4c, d). This technique was applied to ensure we extracted the most representative viewing angle from the images, as many Mapillary images often have poor orientation and irregular camera angles (Fig. 4c, d). Therefore, excluding such

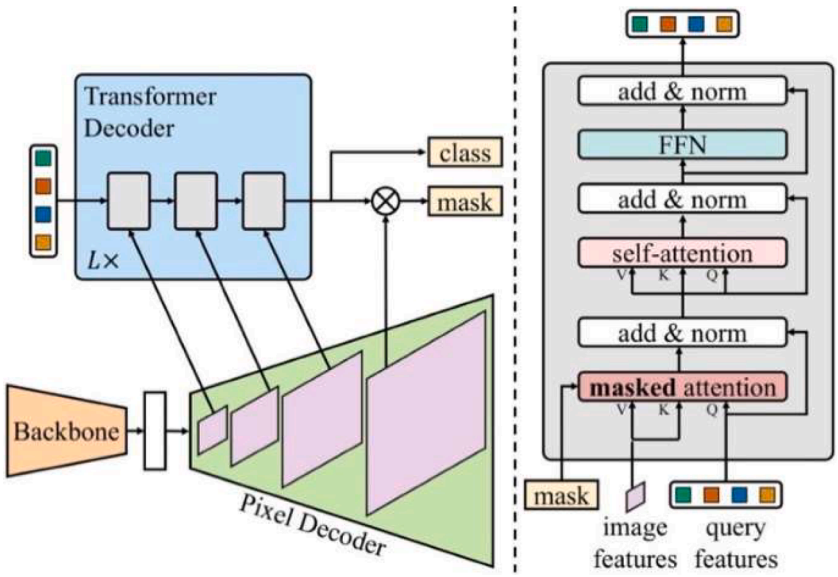

Fig. 3. Mask2Former architecture (Cheng et al., 2022).

images may improve the overall data quality and visibility estimation because irrelevant or less informative images were removed. In cases where an image was both suitable and panoramic, we performed an additional cropping operation (Fig. 4 a1, a2). The image was divided into "N" parts based on the identified road centres (Fig. 2c). This division allowed for a more focused examination of specific sections of the panoramic image and provided a holistic representation of the surrounding area.

2.3.4. Step 4. Calculate GVI

The GVI equation used in this study was based on Eq. (1), proposed by Yang et al. (2009) for evaluating the visibility of urban forests. Their GVI calculates the ratio of the total green area from four pictures taken at a street intersection to the total area of the four pictures.

$$\mathrm{GVI} = \frac{\sum_{i=1}^{4} \mathrm{Area}_{\mathrm{green\_pixels\_i}}}{\sum_{i=1}^{4} \mathrm{Area}_{\mathrm{total\_pixels\_i}}} \cdots \quad (1)$$

Where $\mathrm{Area}_{\mathrm{green\_pixels\_i}}$ represents the count of green pixels in the image captured in the *i*th direction (north, east, south, or west) at a specific intersection, and $\mathrm{Area}_{\mathrm{total\_pixels\_i}}$ corresponds to the total number of pixels in the image captured in the *i*th direction. However, due to the unavailability of images captured in all four directions for all sample points in our dataset, we made a slight modification to the formula. The modified GVI we used can be expressed with Eq. (2).

$$\mathrm{GVI} = \frac{\sum_{i=1}^{N} \frac{\mathrm{Area}_{\mathrm{green\_pixels\_i}}}{\mathrm{Area}_{\mathrm{total\_pixels\_i}}}}{N} \cdots \quad (2)$$

Where $\mathrm{Area}_{\mathrm{green\_pixels\_i}}$ is the number of green pixels in the *i*th picture found in the sample point, $\mathrm{Area}_{\mathrm{total\_pixels\_i}}$ is the total pixel number of the *i*th picture found in the sample point, and N is the number of analysed pictures in the sample point. For non-panoramic images, N is equal to 1 since there is only one image available at the sample point. However, for panoramic images, N corresponds to the number of road centres identified at the sample point, indicating the number of cropped images.

2.4. Evaluate image availability and image usability

In assessing image availability, we examined the presence of an assigned image for each sample point. Any sample point that did not have a corresponding image found within a 25 m buffer was excluded. The availability of images in the dataset is expressed in Eq. (3) as the ratio of the number of sample points with assigned images ($N_{\mathrm{img\_assigned}}$) to the total number of sample points N_{total}.

$$\text{Image Availability Score (IAS)} = \frac{N_{\mathrm{img\_assigned}}}{N_{\mathrm{total}}} \cdots \quad (3)$$

Similarly, in evaluating image usability, we focused on points that had assigned images and a known GVI value. This indicated that the image met the expected criteria for inclusion in the analysis. The quality of the data is represented in Eq. (4) as the ratio of the number of sample points with assigned images and known GVI values ($N_{\mathrm{img\_assigned} \wedge \mathrm{GVI\_known}}$) to the total number of sample points with assigned images ($N_{\mathrm{img\_assigned}}$).

$$\text{Image Usability Score (IUS)} = \frac{N_{\mathrm{img\_assigned} \wedge \mathrm{GVI\_known}}}{N_{\mathrm{img\_assigned}}} \cdots \quad (4)$$

Then, to enable a more meaningful comparison between cities of varying sizes, an adjustment was made to both scores by incorporating the natural logarithm of the road length in kilometres, as shown in Eqs. (5) and (6). By applying this logarithmic transformation, the adjustment places greater emphasis on the relative differences in road lengths between cities, rather than absolute values.

$$\text{Adjusted Image Availability Score (AIAS)} = \frac{N_{\mathrm{img\_assigned}}}{N_{\mathrm{total}}} \times \ln(\mathrm{road\_length}) \cdots \quad (5)$$

$$\text{Adjusted Image Usability Score (AIUS)} = \frac{N_{\mathrm{img\_assigned} \wedge \mathrm{GVI\_known}}}{N_{\mathrm{img\_assigned}}} \times \ln\left(\mathrm{road\_length}\right) \cdots \quad (6)$$

In addition to the availability and usability assessment, we conducted further analysis to provide additional insights. Firstly, we measured the proportion of panoramic images in each city. This assessment allows us to evaluate the availability and coverage of panoramic imagery, which can provide a more comprehensive view of the surrounding locations. Furthermore, we examined the types of roads (e.g., residential, primary, secondary roads) with the most missing images. By identifying the specific road types where the image coverage is limited, we can gain insights into potential gaps in the dataset. This information is valuable for understanding the limitations and areas that require further attention in improving the availability of images for analysis.

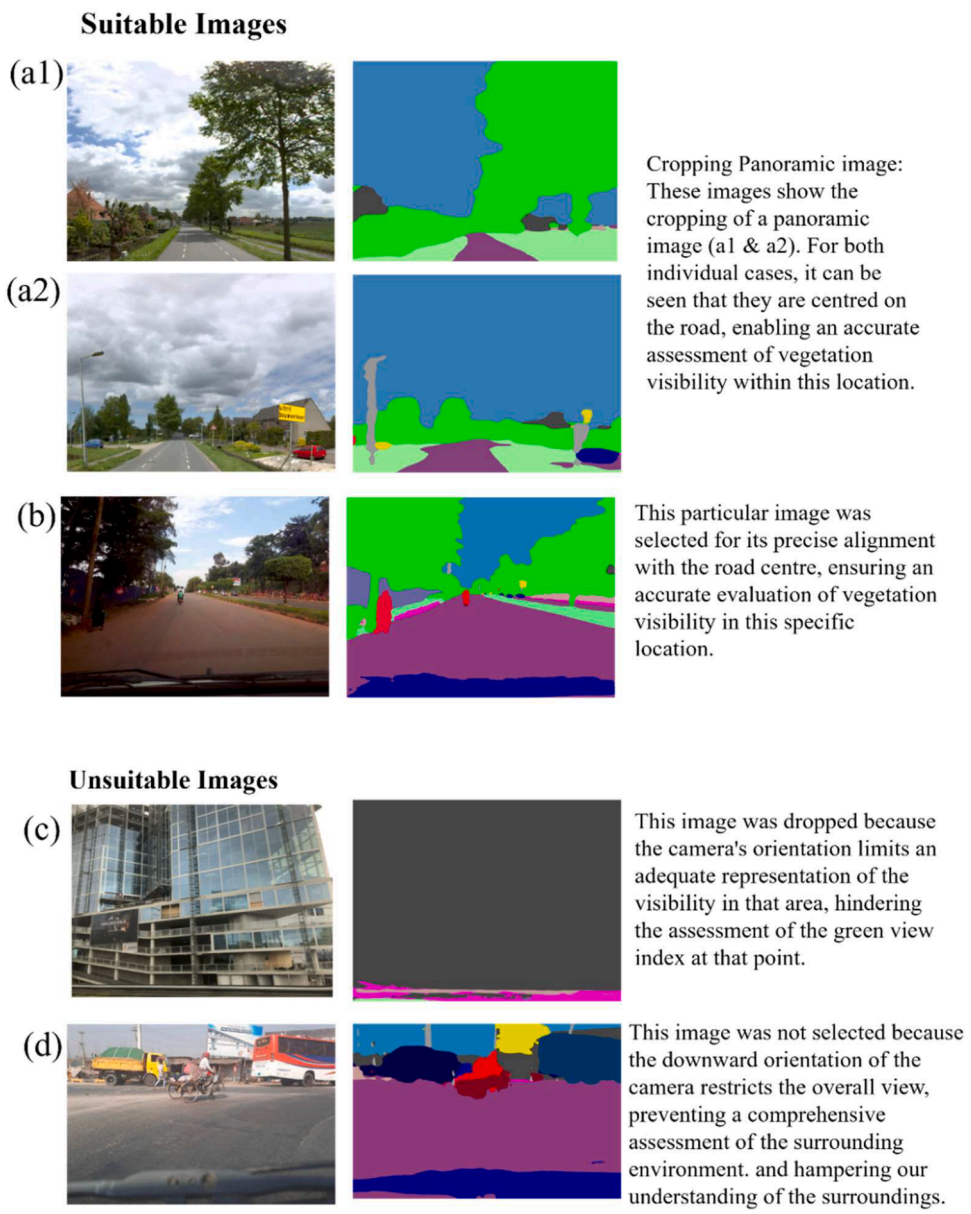

Fig. 4. Example of image segmentation and filtering criteria for suitable image selection.

2.5. Model GVI for missing image points

To estimate the GVI values for the missing data points, we employed two modelling approaches per city: Linear Regression and Linear Generalised Additive Models (GAM). In both cases, we utilised the NDVI raster file of each city. For each point in the dataset, we computed the average NDVI value within a fixed-size buffer surrounding the point. After conducting tests with multiple buffers of 100, 50, and 25 m, it was determined that the buffer of 25 m exhibited the best model performance. Subsequently, we employed the points with known GVI values and their corresponding calculated NDVI values to train both the Linear Regression and the Linear GAM models. The performance of these models was evaluated using the Root Mean Square Error (RMSE) through cross-validation with five folds. Additionally, we computed the Akaike Information Criterion (AIC) score to facilitate a comparison between the two models. Finally, both models allowed us to estimate GVI values based on the available GVI and NDVI data in each city, thereby completing the information for the missing points.

2.6. Computational resources

The data processing and analysis for this study were implemented using the Python programming language. Python provides a wide range of libraries and tools that facilitate the handing and manipulation of de data, as well as the implementation of various algorithms and models. We utilised Google Colab to execute the code. The Google Colab environment provided several advantages, including the availability of a high amount of RAM and GPU acceleration, which significantly contributed to the efficiency of the image segmentation process. For this research, we employed a computational system with 25.5 GB of RAM and a T4 GPU accelerator with a 15 GB memory capacity. This configuration allowed us to handle large datasets and smoothly execute memory-intensive operations, resulting in a substantial reduction in processing time for each image. Additionally, we implemented parallel processing techniques to enhance the efficiency of the image segmentation process and maximise the utilisation of the available computational resources. Through the combination of these implemented techniques and computational resources described above, we achieved

high processing capabilities that enabled us to analyse approximately 4000 images within a span of 40 min.

2.7. Evaluating Mapillary GVI

In order to assess the consistency and reliability of GVI, we compared the GVI values obtained from Mapillary images to those derived from GSV images to evaluate the degree of agreement between both datasets. This comparison was conducted on both city-specific and all-case city levels to provide a comprehensive assessment of our methodology. To evaluate the GVI agreement on a city-specific basis, we sampled 100 random locations in each city. We extracted Mapillary and GSV data on the sample locations using the same methodology in Section 2.3. Then, we computed the Pearson correlation coefficient for each city for these sample locations. The correlation coefficient quantifies the degree of similarity between GVI values derived from Mapillary and GSV images for each city. In addition to this, we also calculated the overall correlation coefficient, encompassing the sample points from all case cities. This aggregate correlation coefficient provides a general measure of the comprehensive assessment of the relation between GVI scores obtained using Mapillary and GSV images. Furthermore, for external validation, we compared our overall Mapillary-driven street-level GVI values with data from MIT's Treepedia project (https://senseable.mit.edu/treepedia) conducted by the Senseable City Lab (Cai et al., 2018; MIT Senseable City Lab, 2023). The Treepedia project utilized Google Street View (GSV) data to model GVI in various cities, including some of the cities in our study (i.e., Amsterdam, Buenos Aires, Kobe, Tel Aviv, and Seattle).

3. Results

3.1. Image availability and image usability of Mapillary data

After designing and implementing the methodology to calculate the GVI using Mapillary data in any city worldwide, we obtained the GVI information for eleven different cities. In order to provide a comprehensive overview of our findings, we will first address Research Question 1, which involves comparing the GVI across different cities and evaluating the availability and usability of image data obtained through Mapillary. Fig. 5 provides a visual representation of the calculated GVI values using exclusively Mapillary image data, highlighting disparities in image availability across the selected cities. As illustrated, Fig. 5a, corresponding to Seattle, Fig. 5b to Barcelona, Fig. 5c to Amsterdam, and Fig. 5k to the City of Melbourne, consistently exhibit the highest degree of image availability. This observation aligns with the high AIAS achieved by cities, as shown in Table 1. On the other hand, our findings reveal a contrasting situation for Ho Chi Minh (Fig. 5g), Buenos Aires (Fig. 5h), Kampala (Fig. 5i), and Dhaka (Fig. 5j) which exhibit considerably lower AIAS compared to cities like Amsterdam and Seattle. Intriguingly, Fig. 5f shows a remarkable disparity in image availability within Mexico City, with its southern region displaying substantially fewer images compared to the central area. Interestingly, Fig. 5e and d show that Kobe and Tel Aviv exhibit a low AIAS (Table 1) compared to other cities that are part of developed countries. Such a pattern highlights that Mapillary has considerable spatial variability in data availability among and between cities.

Regarding the usability, as presented in Table 1, our findings provide intriguing insights into the usability of street-view imagery, adjusted for city size, in our eleven cities of interest. Notably, Ho Chi Minh and

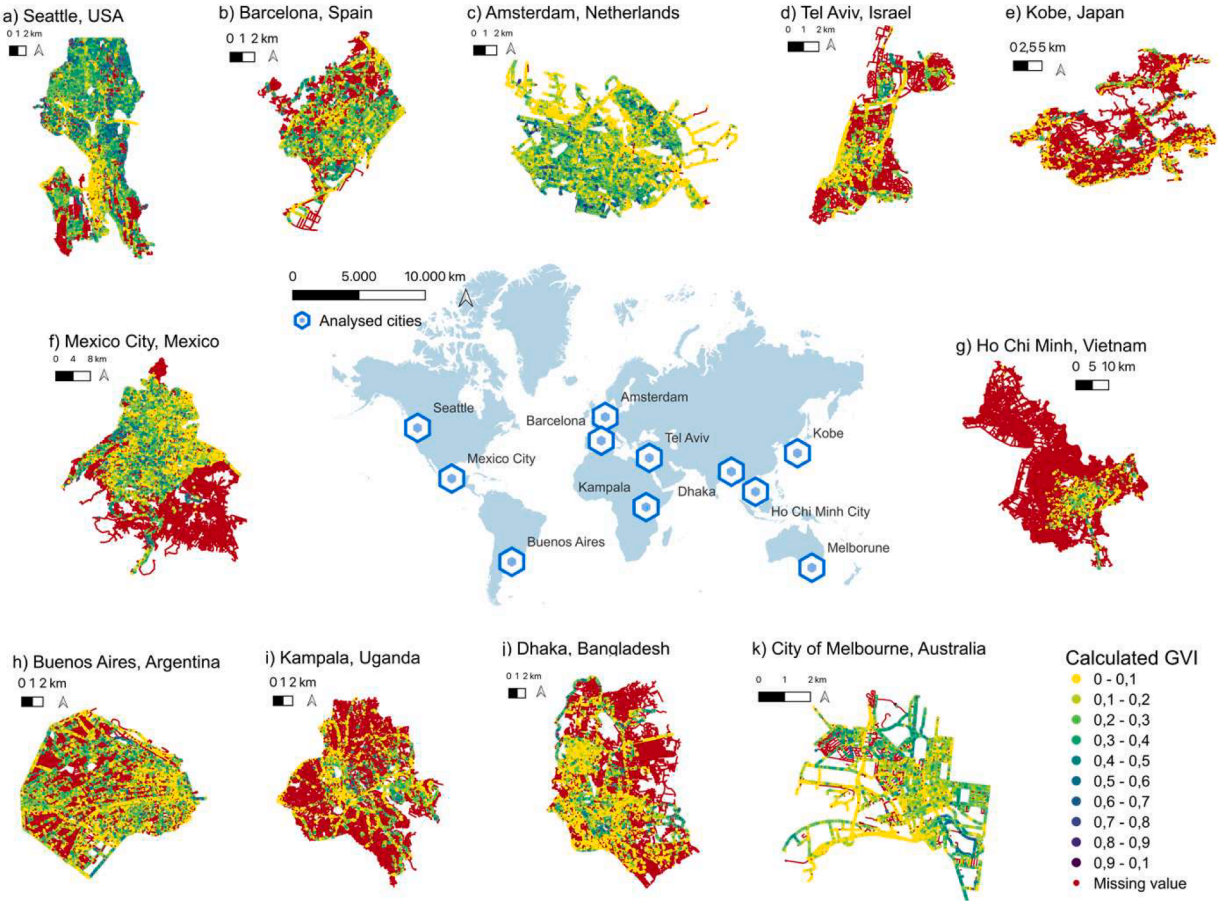

Fig. 5. Calculated GVI across different cities using Mapillary Image Data.

Table 1
Image availability score, adjusted availability score, image usability score and adjusted image usability score for each analysed city.

City	IAS	AIAS	IUS	AIUS
Ho Chi Minh	0.1209	1.3404	0.9531	10.5620
Kobe	0.1749	1.8578	0.8392	8.9114
Tel Aviv	0.3739	3.0118	0.7829	6.3064
Kampala	0.3461	3.1067	0.5499	4.9362
Dhaka	0.3764	3.6895	0.8355	8.1887
Buenos Aires	0.4174	3.9423	0.7807	7.3697
Barcelona	0.5204	4.5773	0.8222	7.2312
Mexico City	0.4468	4.9863	0.8469	9.4514
City of Melbourne	0.8371	6.4510	0.8906	6.8629
Seattle	0.7610	7.2340	0.8271	7.8632
Amsterdam	0.9871	9.2057	0.9570	8.9252

Mexico City stand out with the highest AIUS, suggesting that despite the uneven distribution of image availability, as indicated in Table 1, the proportion of usable images remains high. Similarly, Tel Aviv exhibits a relatively high IUS despite having the lowest availability in Table 1, indicating that although the volume of images in this city was lower, the proportion of usable images was high. Furthermore, Amsterdam once again demonstrates a high AIUS, consistent with its high Image Usability Score. This consistency indicates that the robustness of the usable image data in this city is largely maintained, even after accounting for city size.

In terms of panoramic images, the data presented in Table 2 reveals a considerable difference in the availability of panoramic images. Amsterdam stands out prominently with the highest number, as more than 80 % of its images are panoramic. In contrast, the remaining cities exhibit considerably lower proportions of panoramic images. For instance, Dhaka did not have any panoramic images in its dataset. In contrast, Mexico City, the City of Melbourne, Barcelona, Kampala, Tel Aviv, and Buenos Aires all have approximately 2 % or less of their total images classified as panoramic.

Next, we analysed the presence of missing values in each street of the cities, identifying the top five highway types with the highest number of missing images. Furthermore, we calculated the proportion of missing images corresponding to each category in every city. Our analysis revealed a consistent trend across all cities, with residential streets displaying the highest proportion of missing images, as depicted in Fig. 6. Fig. 6 illustrates that not only do residential streets have the highest volume of missing images in each city, but this deficit is notably significant, with all cities surpassing a 30 % mark. This consistent and substantial percentage underscores a significant data gap within residential areas.

3.2. Modelled GVI for missing points using NDVI

Regarding Research Question 2, the viability of using NDVI to fill in missing data points was assessed by utilising Linear Regression and Linear GAM. Our results, shown in Table 3, reveal some key insights. Across cities, Linear Regression consistently resulted in lower RMSE values compared to Linear GAM, indicating a more accurate model with smaller residuals. The AIC scores highlight a consistent preference for the linear regression models over the linear GAM models across all cities. For instance, in Seattle, the Linear Regression model resulted in an AIC of -161,384.4018, while the Linear GAM model yielded a less effective AIC of -136175.2627. This pattern is repeated across all examined cities, indicating a more favourable balance of fit and simplicity for the Linear Regression models when predicting GVI with NDVI.

Furthermore, Fig. 7 shows the trend line and R-squared values observed across the tested cities, showing a relatively low value for most of them. However, the comparatively lower RMSE values obtained in our study indicate that, despite the low R-squared values suggesting a degree of unexplained variability, the RMSE values provide a more optimistic outlook on the utility of our models for predicting GVI using NDVI.

Fig. 8 provides a visual comparison between missing GVI values and their predictions using Linear Regression models for two contrasting cities: Amsterdam and Kampala. The black squares in the zoomed images show that the predicted GVI values closely align with the calculated GVI values using street-view imagery for the surrounding points in both cities.

Table 2
Proportion of panoramic images for each analysed city.

City	Panoramic Images	Total Images	Proportion
Dhaka	0	31,078	0
Mexico City	689	137,994	0.0049
City of Melbourne	52	8693	0.0059
Barcelona	128	14,993	0.0085
Kampala	197	14,162	0.0139
Tel Aviv	128	6325	0.0202
Buenos Aires	682	28,395	0.0240
Seattle	7069	47,031	0.1503
Kobe	4831	20,125	0.2401
Ho Chi Minh	20,525	30,848	0.6653
Amsterdam	32,216	38,040	0.8468

3.3. Mean and median GVI comparison between cities

For Research Question 3, Fig. 9 provides a visualisation of the mean and median GVI value for each street in the studied cities indicating the differences in street-level greenness visibility between cities. The GVI values show clear variations between developed and developing cities across continents in terms of green visibility. Seattle in North America has a higher value of 30.05 % (Fig. 9a), indicating abundant visible green spaces. In Europe, Amsterdam follows closely with a GVI of 22.38 % (Fig. 9c). However, Asian, and African cities like Dhaka and Kampala have lower GVI values of 16.62 % (Fig. 9j) and 18.52 % (Fig. 9i), respectively. These variations underscore the disparities in green view visibility between developed and developing cities, with the former having a better supply.

3.4. Evaluations of Mapillary GVI

The correlation coefficients presented in Table 4 represent the degree of agreement between GVI values derived from Mapillary images and those obtained from GSV in the exact 100 locations within each city. The cities of Buenos Aires and Kampala demonstrate exceptionally strong and significant positive correlations of 0.6471 and 0.6329, respectively. This suggests a high level of agreement between GVI values from both data sources in these cities. On the other hand, Barcelona and Kobe, while still showing positive correlations, have comparatively weaker values, and for Kobe, the correlation was not statistically significant. These cities exhibit some degree of agreement. However, the low correlation values might be attributed to the availability of Mapillary data. For instance, in Barcelona, our sample has only a few panoramic images, whereas all the GSV images were panoramic. Thus, more green pixels might have been extracted from GSV from multiple directions on the same location compared to unidirectional Mapillary images. Additionally, the Mapillary image availability in Kobe was one of the lowest (Table 1); the sample locations might not obtain enough variability in GVI values. In contrast, several cities, including Seattle, Tel Aviv, Mexico, Ho Chi Minh, Dhaka, and the City of Melbourne, exhibit significant moderate positive correlations ranging from 0.3593 to 0.4645. Finally, we observed a significant strong positive correlation between Mapillary and GSV-driven GVI estimates when all cities are considered together. These results indicate that mapillary data can provide results similar to GSV-based GVI modelling; the reliability of Mapillary GVI would be context-specific and depends on the availability and types of images.

Moreover, for external validation, we compared our estimated

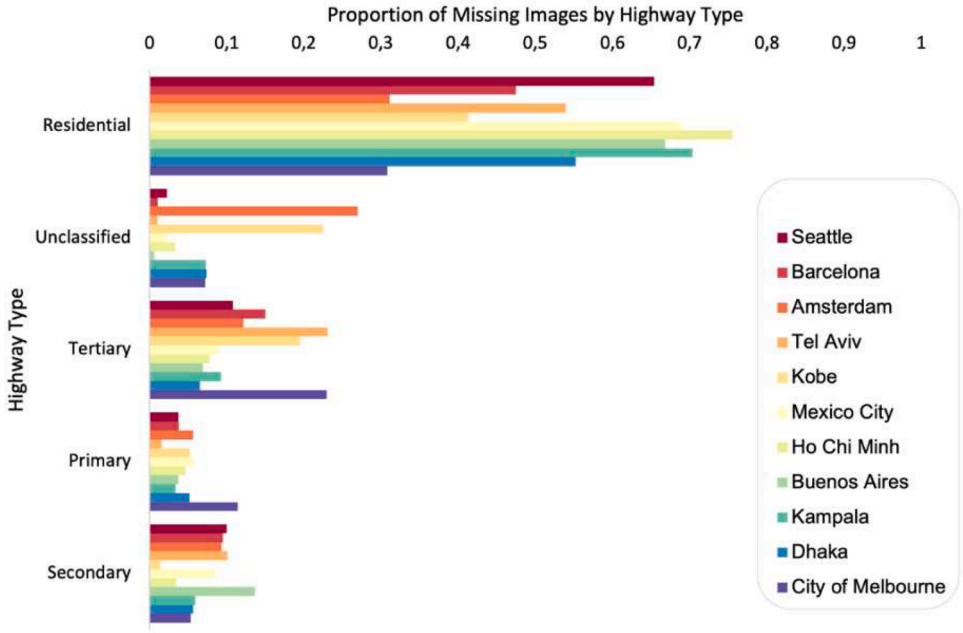

Fig. 6. Top 5 OSM highway types with most missing images.

Table 3
Linear regression and linear GAM model evaluation.

City	Linear Regression		Linear GAM	
	RMSE	AIC	RMSE	AIC
Tel Aviv	0.1271	-20,422.5508	0.1458	-19,060.8670
Kampala	0.1222	-32,733.2024	0.1449	-30,080.0228
Barcelona	0.1291	-50,461.6461	0.1496	-46,833.4747
Kobe	0.1157	-73,035.0463	0.1326	-68,219.0919
Buenos Aires	0.1126	-96,800.8352	0.1339	-89,114.0967
Dhaka	0.1242	-108,314.5968	0.1434	-100,829.2755
Mexico City	0.1239	-488,017.0528	0.1621	-425,206.4704
City of Melbourne	0.1305	-31,516.7640	0.1505	-29,316.2603
Seattle	0.1256	-161,384.4018	0.1737	-136,175.2627
Amsterdam	0.1660	-130,717.0516	0.1832	-123,572.8984
Ho Chi Minh	0.1053	-132,332.5372	0.1249	-122,321.0675

median street-level GVI, and the median city-specific values provided by Treepedia using GSV images (Table 5). Our assessment for cities such as Amsterdam, Buenos Aires, Kobe, and Tel Aviv revealed slight overestimations in our median GVI values compared to Treepedia's estimates. Notably, the disparities in GVI values for these cities generally remained within the range of approximately 3 % or less. Although we used different datasets, the median GVI values are similar to Treepedia's. However, in the case of Seattle, our approach overestimated the overall GVI score by about 10 %. This discrepancy can be attributed to the limited availability of panoramic images in the Mapillary dataset (only 15 % coverage in Seattle) compared to the predominantly panoramic GSV images used by Treepedia. Additionally, our study employed NDVI to estimate GVI in areas where data was missing, which was not implemented in the Treepedia project (Cai et al., 2018). Furthermore, the difference may be attributed to temporal variations in image collection between GSV and Mapillary. The results of our external validation indicate that using Mapillary images can produce similar results to GSV-based GVI estimation, with a reasonable margin of difference between these two datasets.

4. Discussion

4.1. Main findings

In this study, we aimed to develop a methodological framework for utilising open-source image data for greenness visibility modelling and evaluate the completeness and usefulness of such data in multiple cities in different countries worldwide. To the best of our knowledge, no previous studies have developed such a methodology using open-source images (e.g., Mapillary) and implemented similar approaches in diverse geographic contexts. Our study revealed novel insights into using Mapillary data to calculate GVI across different cities, effectively addressing our first research question. We found that image availability, represented by the AIAS, varied significantly among the selected cities. Seattle, Amsterdam, and the City of Melbourne consistently had high image availability. By contrast, cities like Ho Chi Minh, Dhaka, Kobe, and Kampala had much lower scores, as indicated in Fig. 5 and Table 1. For Ho Chi Minh and Kobe, the lower availability of images indicates that in image-scarce contexts, the use of Mapillary for GVI analysis might be restricted, and widespread public effort should be promoted to encourage more image collection. However, interestingly, we found that the usability of images did not necessarily correlate with their volume or image availability. Table 1 shows that despite having fewer images, Mexico City and Tel Aviv had high AIUS, indicating that a large proportion of the available imager was usable. This suggests meaningful GVI assessments are possible for places with usable images even though the city's overall image availability is limited. The distribution of panoramic images also showed a remarkable contrast across cities (Table 2). The disparity could impact the depth and breadth of GVI analysis, as panoramic images typically provide a more comprehensive view of greenery in the surrounding area than a single image with a limited view angle. Furthermore, our study pinpointed a considerable data gap in residential areas. We observed that these areas consistently showed the highest volume of missing images, as illustrated in Fig. 6. This consistent deficit could pose potential challenges for comprehensive GVI assessments, highlighting the need for effective data supplementation methods. Our results are consistent with the previous study by Juhász and Hochmair (2016), who also demonstrated that the availability of images varies considerably between countries and street types.

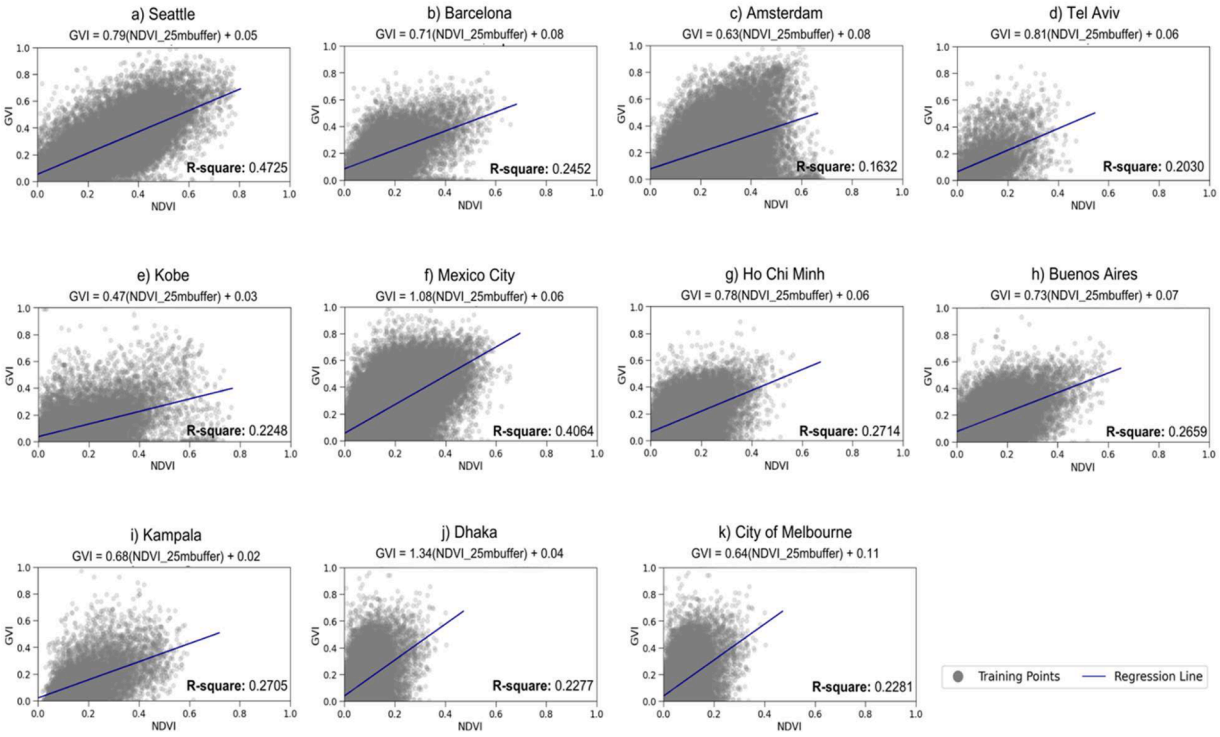

Fig. 7. Linear regression trend lines and equations for each city.

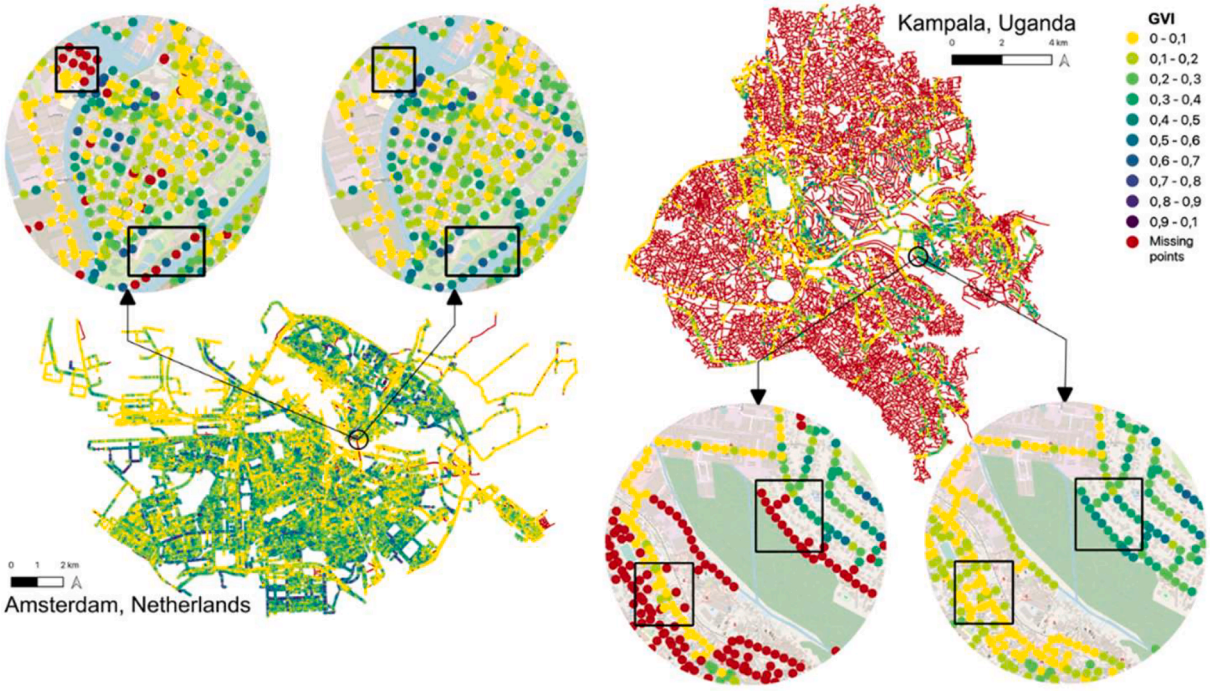

Fig. 8. Comparing image availability between Amsterdam and Kampala, with GVI estimation for missing points using a linear regression model for each city.

Despite having varying image availability and usability scores in different cities, our evaluation of the Mapillary image-driven analysis indicates that, usually, GVI estimated using Mapillary images have positive significant correlations with GVI values estimated utilising Google Street View (GSV) images (Table 4). Moreover, our estimated city-level median GVI values are comparable to the Treepedia project's median GVI values (Table 5). It should be noted that Treepedia used GSV (Cai et al., 2018; Li et al., 2015), whereas utilised open-source images. These insights are critical to argue that considering growing concerns about GSV not adhering to FAIR principles and lacking open-access availability (Rundle et al., 2022), more focus should be given to using VSVI sources by developing innovative methods to increase the usability of such images for GVI estimation with improved accuracy. Additionally, more public efforts and resources should be employed to support and expand VSVI initiatives by protecting existing VSVI images and increasing the quality and consistency of image collection to ensure

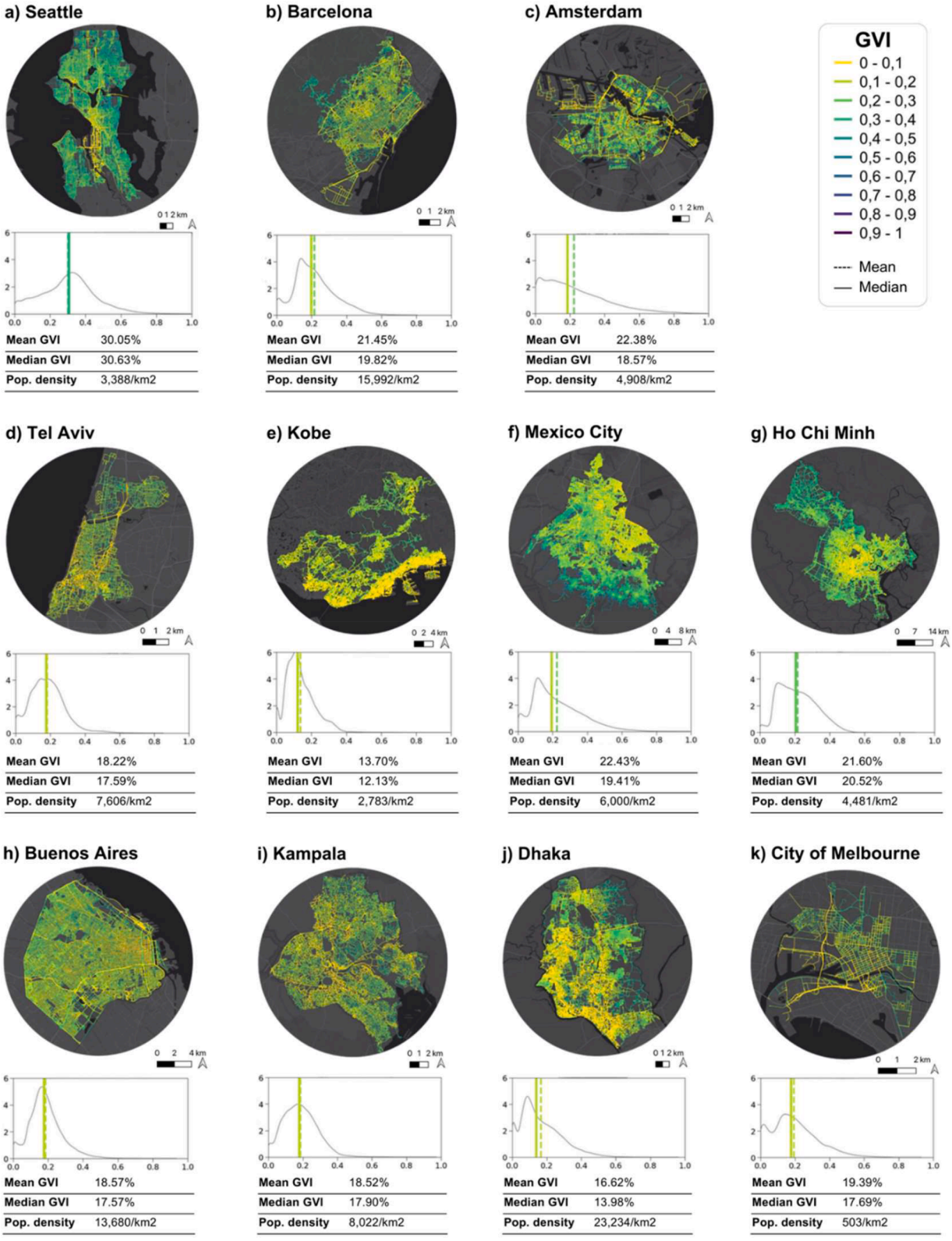

Fig. 9. Mean and Median GVI per city along with their density plot, showing the different levels of street-level greenness visibility in diverse geographical contexts.

VSVI can become a reasonable substitute to commercial street view images.

Addressing our second research question, our analysis also suggests that the NDVI can be used to calibrate a linear regression model for each city to fill in missing GVI data points with reasonable errors. In Fig. 8, we illustrated that even in cities like Kampala, where the number of missing images is significantly high, estimated GVI values from NDVI align closely with those derived from street-view images. We argue that even though NDVI does not directly represent the visibility of greenery, as they indicate the presence of vegetation from a top-down viewing perspective (Labib et al., 2021; Larkin & Hystad, 2019), the modelled relations can reasonably estimate potential GVI values. Moreover,

Table 4
Correlations between Mapillary and GSV image-based GVI values at sample locations.

City	N	Correlation Coefficient
Seattle	100	0.4458**
Barcelona	100	0.2387*
Amsterdam	100	0.3183**
Tel Aviv	100	0.3593**
Kobe	100	0.2069
Mexico City	100	0.4233**
Ho Chi Minh	100	0.4305**
Buenos Aires	100	0.6471**
Kampala	100	0.6329**
Dhaka	100	0.4645**
City of Melbourne	100	0.4606**
All city together	1100	0.6311**

** $p < 0.001$, * < 0.05.

Table 5
Comparisons between Mapillary image based median GVI and Treepedia's estimation.

City	Mapillary median street-level GVI	Treepedia's city-specific GVI
Amsterdam	18.57	20.6
Buenos Aires	17.57	14.5
Kobe	12.13	9.4
Tel Aviv	17.59	17.5
Seattle	30.63	20.0

Torkko et al. (2023) also observed that NDVI values might correspond to perceived visibility greenery. Considering these aspects, accounting for the wider availability of NDVI at varying spatial and temporal resolutions, using NDVI to estimate potential GVI values with reasonable accuracy can be useful in many urban contexts where street view image coverage is limited. However, these results should be interpreted cautiously considering the temporal and spatial mismatch between NDVI and street view images, the potential presence of objects obstructing views (e.g., buildings), the local vegetation types, and topographic contexts.

Finally, for the third research question, our analysis underscores a notable disparity in GVI across cities, particularly in high-density cities in Asia and Africa. As Fig. 9 illustrates, these densely populated, lower-income cities exhibit considerably less green visibility than low-density, high-income cities in the USA and Europe; such results are consistent with Treepedia data. This disparity may be attributed to various factors, including the differences in urbanisation rate, urban planning strategies and investment in public spaces, the socioeconomic development level, as well as the historical and cultural values assigned to green spaces in these regions (Dierwechter, 2017; Mora & Bolici, 2017; Abebe, 2013; Mortoja & Yigitcanlar, 2022).

4.2. Urban planning and policy implications of GVI modelling

The methods and results presented in this study have several applications in urban planning, design, and policy formulation. For instance, urban planners and designers could use maps to pinpoint locations in the city streets where urban greening interventions are most crucial to increase visual contact with greenery. By strategically incorporating trees and other nature-based solutions (e.g., pocket parks, green walls) along transportation routes, cities can positively increase nature exposure as people move within the city, ensuring that transportation systems are not only attractive but also contribute to overall urban greenery, which in turn may reduce the air and noise pollution impacts and lower the high-temperature exposures (Wu et al., 2020; Deng et al., 2023; Nourmohammadi et al., 2021; Song et al., 2023). Our estimated GVI score on each street segment clearly indicates the street to prioritise for such interventions. Furthermore, our results can be valuable for transport planning; for instance, our GVI values can be integrated within transport routing modelling to evaluate and select greener routes for various trips (Willberg et al., 2023; Staves et al., 2023). In addition to these practical implications, our empirical results can also aid in formulating urban greening policies based on cities in different geographic contexts. Our results demonstrated disparities in visible greenery between cities, which can assist in developing new urban greening policies in cities with low vegetation coverage and high pressure of urbanisation. Although the results of GVI and its implications in urban planning are not exclusive to the image data we used in this study, compared to the commercial data (e.g., Google Street View), which often restrict free and large-scale usage of images and does not adhere to the FAIR data principles, we argue that our methods will allow developing free and efficient approaches of using VSVI images to facilitate urban planning policies at large scale while ensuring FAIR principles in the process.

4.3. Strengths and limitations

Our study exhibits multiple strengths that reinforce its relevance within green visibility research. Firstly, it used open-source, free, and FAIR data from Mapillary, making a significant stride in democratising and promoting open science in GVI assessments. Our method considered the vertical aspects of urban vegetation and modelled greenness from a human perspective, which provides an improved way to estimate greenness compared to the top-down measures of greenness based on satellite and land use datasets (Larkin & Hystad, 2019; Labib et al., 2020b). We also demonstrated that the GVI estimated in this study could be comparable to results produced by commercial Google Street View data, which pose financial constraints and exclusion in using such data. Our method establishes an example for subsequent research, highlighting the effectiveness of open data for scientific purposes. Secondly, the scalability of the designed methodology in our research is a noteworthy aspect. Our approach to calculating GVI is not confined to the selected cities but can be replicated and scaled for any city worldwide. This scalability is particularly significant considering the growing need for GVI assessments in urban spaces, particularly in cities in the global south, where similar studies are rarely conducted. Thirdly, our innovative approach to modelling visibility by combining GVI and NDVI represents a step forward in the field. By using NDVI and known GVI points, we developed models that allow us to fill in the missing GVI data points in a city; we provide a novel solution that holds the potential to expand and enhance the depth of GVI studies, even in contexts where street-view imagery data may be limited. Fourthly, it is important to emphasise that the code used in this study is reproducible. The implemented code is publicly available, encouraging transparency, peer verification, and further innovation in the field. Reproducibility reinforces the validity of our findings and empowers other researchers to build upon our work, advancing our collective understanding of urban green spaces and human well-being.

Nevertheless, our research had certain limitations that need to be acknowledged for a comprehensive understanding of our results. Despite the utility of Mapillary, we encountered poor image availability in Dhaka, Kampala, Mexico City, Tel Aviv, Kobe, and Ho Chi Minh which can limit the assessment of GVI solely with Mapillary street-view images. However, Amsterdam, City of Melbourne, and Seattle exhibited a more favourable situation regarding image availability. These disparities in image availability can be attributed to the socioeconomic backgrounds of the cities (Fry et al., 2020), which may potentially lead to a less engaged community contributing to a crowd-sourced database. Also, it is important to note that user-contributed images on platforms such as Mapillary exhibit significant variability in image quality, which can be linked to factors like lighting conditions, camera equipment specifications, and image resolutions (Ma et al., 2020). As a result, even though our study employed a segmentation algorithm to assess image usability based on image orientation and camera angles, other image quality concerns, including variations in lighting, blurriness, and distortion,

could have influenced the quality of retained images and thus might have impacted the GVI estimation (Zheng & Amemiya, 2023).

Furthermore, our method relies on the assumption that interference factors are minimized due to the way we sampled locations on streets to capture images. In this approach, we utilise selected images at intervals of 50 m, which allows us to collect multiple viewing perspectives from the same location, facilitating the analysis of the same area from different angles and viewpoints. This multi-perspective approach can reveal details that might be missed in a single image due to obstructive features (e.g., cars, persons). However, it does not eliminate potential interference factors efficiently, which requires further development of our method.

Another considerable limitation was the temporal nature of our study, given that the Mapillary data were sourced at a specific point in time, and it may not be updated frequently or uniformly. The dynamic character of crowd-sourcing databases could mean that the image data might have been augmented, updated, or even rendered obsolete since our data collection. However, these issues are not exclusively to Mapillary; even GSV imagery exhibits significant variability in availability and quality (Biljecki & Ito, 2021; Hara et al., 2013). Further, the infrequent updating of images impedes temporal assessment, as certain regions may remain unchanged for years (Hara et al., 2013). Such limitations are particularly evident in lower-income regions, rural areas, and countries in Africa, South America, and Southeast Asia, where GSV imagery remains unavailable or limited (Biljecki & Ito, 2021; Rzotkiewicz et al., 2018). An additional limitation regarding the temporal nature of our study relates to the inherent disparities in seasons, climates, and other contextual factors existing across the different cities at the same point in time. The timing of our data collection spans various geographic locations, each with its own unique seasonal patterns and climatic conditions. This temporal divergence can introduce some effects that must be considered. For instance, varying seasons and climatic factors can result in distinct states of urban greenery. During spring and summer months, cities may exhibit lush greenery, while the fall and winter seasons may see a reduction in green cover. Such phenological patterns could vary considerably depending on the cities' location and climate zones (Gardner et al., 2020; Rathcke & Lacey, 1985). The presence of different seasons and climates among the selected cities may pose challenges when extracting the best images for GVI modelling and comparing their GVI results across cities.

Moreover, a few specific limitations of using OSMnx for urban studies have been identified. One limitation is related to data availability and consistency, which are recurrent issues in urban planning and street network analysis literature (Boeing, 2017). The data used by OSMnx, sourced from OpenStreetMap (Boeing, 2017), is provided by a community of contributors and, thus, might not always be consistent or up-to-date. This means that any changes to the street networks that have occurred since the last update would not be reflected in the analysis. Furthermore, the reliance on OSMnx data quality and accuracy can vary considerably based on the location. The coverage of OSMnx is good across the United States and Europe, but developing countries might have less thorough street network coverage (Boeing, 2017).

Finally, while our study presented the use of NDVI to fill in missing GVI data points effectively, this approach is not devoid of challenges. NDVI primarily quantifies vegetation from bird's eye view and may not fully capture the nuances of human perception of greenery (Labib et al., 2021; Larkin & Hystad, 2019), which is central to GVI. Thus, utilising NDVI to calculate missing GVI data points could introduce inherent errors, such as the temporal mismatch between satellite and street view images used to estimate NDVI and GVI. This might lead to over or underestimation of modelled GVI values in the missing location based on NDVI images used and surrounding built environment contexts.

4.4. Future research

While this study has provided valuable insights into the usability of Mapillary data for calculating GVI, there are several promising avenues for further investigation. One potential area of investigation is obtaining a weighted average GVI value using population density in determined areas, which can provide a more accurate reflection of green visibility within a city. This approach can provide a more precise depiction of green visibility within a city, considering areas where the presence of greenery might be less perceptible due to low or negligible population density. In addition to recognising the positive impact of green spaces on well-being, research has also highlighted the potential of blue spaces, such as bodies of water, in promoting human health (Labib et al., 2020b; McDougall et al., 2020). Therefore, exploring the feasibility of integrating Mapillary data to calculate the Blue View Index for cities would be valuable. This integration would enable researchers to investigate the influence of both green and blue spaces on various health indicators, providing a more comprehensive understanding of the relationships between urban environments, natural features, and human well-being (Markevych et al., 2017).

Furthermore, to improve the estimation of GVI for missing points using mean NDVI values, it is worth considering the inclusion of more variables, such as building density, height, and orientation. However, such building data are primarily unavailable globally, but more and more data on buildings, such as OSM buildings and Microsoft Building Footprints, are becoming available. Finally, to improve the consistency between street-view images and satellite-derived NDVI data and ensure data comparability across different cities for GVI comparisons, a viable approach can be to filter images based on their capture timestamp to account for seasonal variations. This method holds the potential to improve the quality of our analysis by aligning the timing of street-level image data more closely with the corresponding environmental conditions reflected in the NDVI data. Additionally, future studies should employ new approaches to select images with higher quality and consistency. For instance, further studies can use images of a specific resolution or only select images from a certain camera if sufficient images are available in the study area to ensure that chosen images have consistent and comparable image quality. Exploring these future research directions will not only expand upon the findings of this study and improve the robustness and reliability of this research but also contribute to the development of approaches for urban planning and public health interventions.

5. Conclusions

This research has developed and demonstrated a scalable, reproducible framework for utilising open-source and FAIR Mapillary image data to assess greenness visibility in diverse geographical contexts. Importantly, this research effectively addressed its research questions, demonstrating that despite variations in image availability across different cities, a robust methodology for GVI assessment can be established using images from Mapillary. Our study identified disparities in Mapillary data availability and usability across the selected global cities, bringing to light an uneven global distribution of open-source and free image data. Nonetheless, these disparities did not diminish the potential of Mapillary for GVI evaluations. Additionally, our findings accentuate Mapillary's adherence to FAIR principles, an asset in scientific research in this domain. This feature makes Mapillary an advantageous free and FAIR alternative to Google Street View for GVI assessments despite the discrepancies and temporal limitations that are not only inherent to crowd-sourced data. Our methodology enables new avenues to make urban greenness analysis accessible to all. A key innovation of our study was using globally available NDVI data to estimate GVI values at missing locations. Although not without limitations, this approach proved to be a promising method for augmenting street-level GVI analyses in data-scarce areas. The successful application of NDVI in our study paves the way for future research to refine and expand on this method, further enhancing the robustness of GVI analyses.

Additionally, this study provided a comparative analysis between

cities of varying socioeconomic contexts, finding a notably lesser greener visibility in densely populated, lower-income cities in Asia and Africa as compared to their low-density, affluent counterparts in the USA and Europe. Overall, this study is a critical contribution to urban planning and environmental research, providing an accessible, scalable, and innovative approach to greenness visibility assessment. Our findings and established framework, founded on open-source data and reproducibility, facilitate comparative studies, and establish guidelines for green view assessments across the globe using free images. Through this, we hope to foster a greater understanding of the relationships between urban natural environments and human well-being, driving toward healthier, more equitable, and sustainable cities.

CRediT authorship contribution statement

Ilse Abril Vázquez Sánchez: Data curation, Formal analysis, Methodology, Software, Validation, Visualization, Writing – original draft. **S.M. Labib:** Conceptualization, Methodology, Data curation, Resources, Investigation, Visualization, Writing – original draft, Writing – review & editing, Supervision.

Declaration of competing interest

The authors declare that they have no known competing financial interests or personal relationships that could have appeared to influence the work reported in this paper.

Data availability

Data will be made available on request.

Acknowledgment

The authors would like to thank the anonymous reviewers and editor of this paper for their constructive comments and suggestions. We acknowledge the coding approach-related suggestions of Dr Matthew Danish. Thanks to Dr. Simon Scheider at SGPL, UU, for earlier comments and suggestions to improve the quality of the work. Finally, we appreciate the overall support of the Spatial Data Science and Geo-Intelligence Lab members for their technical discussion and coding sessions.

The data and code of this research are based on open-source platforms, and all of the results can be re-created using reproducible coding workflow outlined in GitHub Repository at https://github.com/Spatial-Data-Science-and-GEO-AI-Lab/StreetView-NatureVisibility. However, if you want to use the GVI outputs produced for case cities, please email Dr. SM Labib.

References

Aguilar, A. G., & Lopez, F. M. (2018). The city-region of Mexico City: Social inequality and a vacuum in development planning. *International Development Planning Review, 40*(1), 51–74. https://doi.org/10.3828/idpr.2018.3

Aikoh, T., Homma, R., & Abe, Y. (2023). Comparing conventional manual measurement of the Green View Index with modern automatic methods using Google Street View and semantic segmentation. *Urban Forestry & Urban Greening, 80*, Article 127845. https://doi.org/10.1016/j.ufug.2023.127845

Akbari, H., Pomerantz, M., & Taha, H. (2001). Cool surfaces and shade trees to reduce energy use and improve air quality in urban areas. *Solar Energy, 70*(3), 295–310. https://doi.org/10.1016/S0038-092X(00)00089-X

Alonzo, M., Bookhagen, B., & Roberts, D. A. (2014). Urban tree species mapping using hyperspectral and lidar data fusion. *Remote Sensing of Environment, 148*, 70–83. https://doi.org/10.1016/j.rse.2014.03.018

Alvarez Leon, L. F., & Quinn, S. (2019). The value of crowd-sourced street-level imagery: Examining the shifting property regimes of OpenStreetCam and Mapillary. *GeoJournal, 84*(2), 395–414. https://doi.org/10.1007/s10708-018-9865-4

Antequera, M. L., Gargallo, P., Hofinger, M., Bulò, S. R., Kuang, Y., & Kontschieder, P. (2020). Mapillary planet-scale depth dataset. A. Vedaldi, H. Bischof, T. Brox, & J.-M. Frahm (Eds.). *Computer vision – ECCV 2020* (pp. 589–604). Springer International Publishing. https://doi.org/10.1007/978-3-030-58536-5_35.

Armson, D., Stringer, P., & Ennos, A. R. (2013). The effect of street trees and amenity grass on urban surface water runoff in Manchester, UK. *Urban Forestry & Urban Greening, 12*(3), 282–286. https://doi.org/10.1016/j.ufug.2013.04.001

Attal, E., Dubus, B., Leblois, T., & Cretin, B. (2021). An optimal dimensioning method of a green wall structure for noise pollution reduction. *Building and Environment, 187*, Article 107362. https://doi.org/10.1016/j.buildenv.2020.107362

Bain, L., Gray, B., & Rodgers, D. (2012). *Living streets: Strategies for crafting public space.* John Wiley & Sons.

Batlle, J., Casals, A., Freixenet, J., & Martí, J. (2000). A review on strategies for recognizing natural objects in colour images of outdoor scenes. *Image and Vision Computing, 18*(6), 515–530. https://doi.org/10.1016/S0262-8856(99)00040-2

Berland, A., Shiflett, S. A., Shuster, W. D., Garmestani, A. S., Goddard, H. C., Herrmann, D. L., & Hopton, M. E. (2017). The role of trees in urban stormwater management. *Landscape and Urban Planning, 162*, 167–177. https://doi.org/10.1016/j.landurbplan.2017.02.017

Biljecki, F., & Ito, K. (2021). Street view imagery in urban analytics and GIS: A review. *Landscape and Urban Planning, 215*, Article 104217. https://doi.org/10.1016/j.landurbplan.2021.104217

Boeing, G. (2017). OSMnx: New methods for acquiring, constructing, analyzing, and visualizing complex street networks. *Computers, Environment and Urban Systems,, 65*, 126–139. https://doi.org/10.1016/j.compenvurbsys.2017.05.004

Bush, J., Ashley, G., Foster, B., & Hall, G. (2021). Integrating Green Infrastructure into urban planning: Developing Melbourne's Green Factor Tool. *Urban Planning, 6*, 20–31. https://doi.org/10.17645/up.v6i1.3515

Cai, B. Y., Li, X., Seiferling, I., & Ratti, C. (2018, July). *Treepedia 2.0: applying deep learning for large-scale quantification of urban tree cover* (pp. 49–56). IEEE.

Chen, J., Zhou, C., & Li, F. (2020). Quantifying the green view indicator for assessing urban greening quality: An analysis based on Internet-crawling street view data. *Ecological Indicators, 113*, Article 106192. https://doi.org/10.1016/j.ecolind.2020.106192

Chen, S., & Biljecki, F. (2023). Automatic assessment of public open spaces using street view imagery. *Cities, 137*, Article 104329. https://doi.org/10.1016/j.cities.2023.104329

Chen, X., Meng, Q., Hu, D., Zhang, L., & Yang, J. (2019). Evaluating greenery around streets using baidu panoramic street view images and the panoramic Green View Index. *Forests, 10*(12), 1109.

Cheng, B., Misra, I., Schwing, A. G., Kirillov, A., & Girdhar, R. (2022). Masked-attention mask transformer for universal image segmentation. In *Proceedings of the 2022 IEEE/CVF conference on computer vision and pattern recognition (CVPR)* (pp. 1280–1289). https://doi.org/10.1109/CVPR52688.2022.00135

Corbane, C., Politis, P., Kempeneers, P., Simonetti, D., Soille, P., Burger, A., & Kemper, T. (2020). A global cloud free pixel- based image composite from Sentinel-2 data. *Data in Brief, 31*, Article 105737. https://doi.org/10.1016/j.dib.2020.105737

D'Andrimont, R., Yordanov, M., Lemoine, G., Yoong, J., Nikel, K., & Van der Velde, M. (2018). Crowd-sourced street-level imagery as a potential source of *in-situ* data for crop monitoring. *Land, 7*(4). https://doi.org/10.3390/land7040127. Article 4.

Deng, X., Gao, F., Liao, S., & Li, S. (2023). Unraveling the association between the built environment and air pollution from a geospatial perspective. *Journal of Cleaner Production, 386*, Article 135768. https://doi.org/10.1016/J.JCLEPRO.2022.135768

Dierwechter, Y. (2017). *Urban sustainability through smart growth: Intercurrence, planning, and geographies of regional development across Greater Seattle.* Springer. https://link.springer.com/content/pdf/10.1007/978-3-319-54448-9.pdf.

Dong, R., Zhang, Y., & Zhao, J. (2018). How green are the streets within the sixth ring road of Beijing? An analysis based on tencent street view pictures and the Green View Index. *International Journal of Environmental Research and Public Health, 15*(7). https://doi.org/10.3390/ijerph15071367. Article 7.

Downs, R. M., & Stea, D. (1977). *Maps in minds: Reflections on cognitive mapping.* Harper and Row.

Edson, C., & Wing, M. G. (2011). Airborne Light Detection and Ranging (LiDAR) for individual tree stem location, height, and biomass measurements. *Remote Sensing, 3*(11). https://doi.org/10.3390/rs3112494. Article 11.

Ellaway, A., Macintyre, S., & Bonnefoy, X. (2005). Graffiti, greenery, and obesity in adults: Secondary analysis of European cross sectional survey. *BMJ, 331*(7517), 611–612. https://doi.org/10.1136/bmj.38575.664549.F7

Falfán, I., Muñoz-Robles, C. A., Bonilla-Moheno, M., & MacGregor-Fors, I. (2018). Can you really see 'green'? Assessing physical and self-reported measurements of urban greenery. *Urban Forestry & Urban Greening, 36*, 13–21. https://doi.org/10.1016/j.ufug.2018.08.016

Abebe, G.A. (2013). *Quantifying urban growth pattern in developing countries using remote sensing and spatial metrics: A case study in Kampala, Uganda* (Master's thesis, University of Twente). http://essay.utwente.nl/84729/1/abebe.pdf.

Fry, D., Mooney, S. J., Rodríguez, D. A., Caiaffa, W. T., & Lovasi, G. S. (2020). Assessing Google Street View image availability in Latin American cities. *Journal of Urban Health, 97*(4), 552–560. https://doi.org/10.1007/s11524-019-00408-7

Gardner, A. S., Maclean, I. M., & Gaston, K. J. (2020). A new system to classify global climate zones based on plant physiology and using high temporal resolution climate data. *Journal of Biogeography, 47*(10), 2091–2101. https://doi.org/10.1111/jbi.13927

Gómez-Baggethun, E., & Barton, D. N. (2013). Classifying and valuing ecosystem services for urban planning. *Ecological Economics, 86*, 235–245. https://doi.org/10.1016/j.ecolecon.2012.08.019

Google. (2018a). Google maps APIs terms of service. Google for developers. https://developers.google.com/maps/terms-20180207?hl=es-4191 August 2023.

Google. (2018b). Google maps, Google earth, and street view. https://about.google/brand-resource-center/products-and-services/geo-guidelines/ 1 August 2023.

Google. (2020). Google maps platform terms of service. Google cloud. https://cloud.google.com/maps-platform/terms; Last Accessed: 1 August, 2023.
Google. (2023). Google maps platform pricing. Google for developers. https://developers.google.com/maps/billing-and-pricing/pricing; Last Accessed: 1 August, 2023.
Gupta, K., Kumar, P., Pathan, S. K., & Sharma, K. P. (2012). Urban neighborhood Green Index – A measure of green spaces in urban areas. *Landscape and Urban Planning, 105*(3), 325–335. https://doi.org/10.1016/j.landurbplan.2012.01.003
Hara, K., Le, V., & Froehlich, J. (2013). Combining crowd-sourcing and Google Street View to identify street-level accessibility problems. In *Proceedings of the SIGCHI conference on human factors in computing systems* (pp. 631–640). https://doi.org/10.1145/2470654.2470744
Helbich, M., Yao, Y., Liu, Y., Zhang, J., Liu, P., & Wang, R. (2019). Using deep learning to examine street view green and blue spaces and their associations with geriatric depression in Beijing, China. *Environment International, 126*, 107–117. https://doi.org/10.1016/j.envint.2019.02.013
Herscovici, A., Dahan, G., & Cohen, G. (2022). Smart cities and tourism: The case of Tel Aviv-Yafo. *Sustainability, 14*(17). https://doi.org/10.3390/su141710968. Article 17.
Inoue, T., Manabe, R., Murayama, A., & Koizumi, H. (2022). Landscape value in urban neighborhoods: A pilot analysis using street-level images. *Landscape and Urban Planning, 221*, Article 104357. https://doi.org/10.1016/j.landurbplan.2022.104357
Jim, C. Y., & Chen, W. Y. (2008). Assessing the ecosystem service of air pollutant removal by urban trees in Guangzhou (China). *Journal of Environmental Management, 88*(4), 665–676. https://doi.org/10.1016/j.jenvman.2007.03.035
Jimenez, M. P., Suel, E., Rifas-Shiman, S. L., Hystad, P., Larkin, A., Hankey, S., & See Acknowledgments for full listing of collaborators. (2022). Street-view greenspace exposure and objective sleep characteristics among children. *Environmental Research, 214*(Pt 1), Article 113744. https://doi.org/10.1016/j.envres.2022.113744
Juhász, L., & Hochmair, H. H. (2016). User contribution patterns and completeness evaluation of Mapillary, a crowd-sourced street level photo service. *Transactions in GIS, 20*(6), 925–947. https://doi.org/10.1111/tgis.12190
Kaplan, S. (1995). The restorative benefits of nature: Toward an integrative framework. *Journal of Environmental Psychology, 15*(3), 169–182. https://doi.org/10.1016/0272-4944(95)90001-2
Keeley, M. (2011). The green area ratio: An urban site sustainability metric. *Journal of Environmental Planning and Management, 54*(7), 937–958. https://doi.org/10.1080/09640568.2010.547681
Ki, D., & Lee, S. (2021). Analyzing the effects of Green View Index of neighborhood streets on walking time using Google Street View and deep learning. *Landscape and Urban Planning, 205*, Article 103920. https://doi.org/10.1016/j.landurbplan.2020.103920
Kido, D., Fukuda, T., & Yabuki, N. (2021). Assessing future landscapes using enhanced mixed reality with semantic segmentation by deep learning. *Advanced Engineering Informatics, 48*, Article 101281. https://doi.org/10.1016/j.aei.2021.101281
Krylov, V. A., & Dahyot, R (2019). Object geolocation from crowd-sourced street level imagery. C. Alzate, A. Monreale, H. Assem, A. Bifet, T. S. Buda, B. Caglayan, B. Drury, E. García-Martín, R. Gavaldà, I. Koprinska, S. Kramer, N. Lavesson, M. Madden, I. Molloy, M.-I. Nicolae, & M. Sinn (Eds.). *ECML PKDD 2018 workshops* (pp. 79–83). Springer International Publishing. https://doi.org/10.1007/978-3-030-13453-2_7.
Labib, S. M., Huck, J. J., & Lindley, S. (2021). Modelling and mapping eye-level greenness visibility exposure using multi-source data at high spatial resolutions. *Science of the Total Environment, 755*, Article 143050. https://doi.org/10.1016/j.scitotenv.2020.143050
Labib, S. M., Shuvo, F. K., HEM Browning, M., & Rigolon, A (2020a). Noncommunicable diseases, park prescriptions, and urban green space use patterns in a global south context: The case of Dhaka, Bangladesh. *International Journal of Environmental Research and Public Health, 17*(11), 3900. https://doi.org/10.3390/ijerph17113900
Labib, S. M., Lindley, S., & Huck, J. J. (2020b). Spatial dimensions of the influence of urban green-blue spaces on human health: A systematic review. *Environmental Research, 180*, Article 108869. https://doi.org/10.1016/j.envres.2019.108869
Labib, S. M., & Harris, A. (2018). The potentials of Sentinel-2 and LandSat-8 data in Green Infrastructure extraction, using object based image analysis (OBIA) method. *European Journal of Remote Sensing, 51*(1), 231–240. https://doi.org/10.1080/22797254.2017.1419441
Lafortezza, R., Carrus, G., Sanesi, G., & Davies, C. (2009). Benefits and well-being perceived by people visiting green spaces in periods of heat stress. *Urban Forestry & Urban Greening, 8*(2), 97–108. https://doi.org/10.1016/j.ufug.2009.02.003
Larkin, A., & Hystad, P. (2019). Evaluating street view exposure measures of visible green space for health research. *Journal of Exposure Science & Environmental Epidemiology, 29*(4). https://doi.org/10.1038/s41370-018-0017-1. Article 4.
Li, X., Zhang, C., Li, W., Kuzovkina, Y. A., & Weiner, D. (2015a). Who lives in greener neighborhoods? The distribution of street greenery and its association with residents' socioeconomic conditions in Hartford, Connecticut, USA. *Urban Forestry & Urban Greening, 14*(4), 751–759. https://doi.org/10.1016/j.ufug.2015.07.006
Li, X., Zhang, C., Li, W., Ricard, R., Meng, Q., & Zhang, W. (2015b). Assessing street-level urban greenery using Google Street View and a modified Green View Index. *Urban Forestry & Urban Greening, 14*(3), 675–685. https://doi.org/10.1016/j.ufug.2015.06.006
Liang, Y., D'Uva, D., Scandiffio, A., & Rolando, A (2022). The more walkable, the more livable? – Can urban attractiveness improve urban vitality? *Transportation Research Procedia, 60*, 322–329. https://doi.org/10.1016/j.trpro.2021.12.042
Lindemann-Matthies, P., & Brieger, H. (2016). Does urban gardening increase aesthetic quality of urban areas? A case study from Germany. *Urban Forestry & Urban Greening, 17*, 33–41. https://doi.org/10.1016/j.ufug.2016.03.010
Long, Y., & Liu, L. (2017). How green are the streets? An analysis for central areas of Chinese cities using Tencent Street View. *PloS One, 12*(2), Article e0171110. https://doi.org/10.1371/journal.pone.0171110
Lu, Y., Ferranti, E. J. S., Chapman, L., & Pfrang, C. (2023). Assessing urban greenery by harvesting street view data: A review. *Urban Forestry & Urban Greening, 83*, Article 127917. https://doi.org/10.1016/j.ufug.2023.127917
Lu, Y., Sarkar, C., & Xiao, Y. (2018). The effect of street-level greenery on walking behavior: Evidence from Hong Kong. *Social Science & Medicine, 208*, 41–49. https://doi.org/10.1016/j.socscimed.2018.05.022
Ma, D., Fan, H., Li, W., & Ding, X. (2020). The State of Mapillary: An exploratory analysis. *ISPRS International Journal of Geo-Information, 9*(1). https://doi.org/10.3390/ijgi9010010. Article 1.
Mapbox. (2023). Vector tiles standards (Tilesets). Mapbox. https://docs.mapbox.com/data/tilesets/guides/vector-tiles-standards/; Last accessed: 1 August 2023.
Markevych, I., Schoierer, J., Hartig, T., Chudnovsky, A., Hystad, P., Dzhambov, A. M., & Lupp, G. (2017). Exploring pathways linking greenspace to health: Theoretical and methodological guidance. *Environmental Research, 158*, 301–317. https://doi.org/10.1016/j.envres.2017.06.028
Martinez, A., & Labib, S. M. (2023). Demystifying normalized difference vegetation index (NDVI) for greenness exposure assessments and policy interventions in urban greening. *Environmental Research, 220*, Article 115155. https://doi.org/10.1016/j.envres.2022.115155
McDougall, C. W., Quilliam, R. S., Hanley, N., & Oliver, D. M. (2020). Freshwater blue space and population health: An emerging research agenda. *Science of the Total Environment, 737*, Article 140196. https://doi.org/10.1016/j.scitotenv.2020.140196
Meitner, M. J. (2004). Scenic beauty of river views in the Grand Canyon: Relating perceptual judgments to locations. *Landscape and Urban Planning, 68*(1), 3–13. https://doi.org/10.1016/S0169-2046(03)00115-4
Meraner, A., Ebel, P., Zhu, X., & Schmitt, M. (2020). Cloud removal in Sentinel-2 imagery using a deep residual neural network and SAR-optical data fusion. *ISPRS Journal of Photogrammetry and Remote Sensing, 166*, 333–346. https://doi.org/10.1016/j.isprsjprs.2020.05.013
Mapillary. (2021, June 21). Mapillary API documentation. https://www.mapillary.com/developer/api-documentation?locale=es_ES; Last accessed: 1 August 2023.
MIT Senseable City Lab. (2023). Treepedia. Treepedia: MIT senseable city lab. http://senseable.mit.edu/treepedia.
Mora, L., & Bolici, R. (2017). How to become a smart city: Learning from Amsterdam. A. Bisello, D. Vettorato, R. Stephens, & P. Elisei (Eds.). *Smart and sustainable planning for cities and regions: Results of SSPCR 2015* (pp. 251–266). Springer International Publishing. https://doi.org/10.1007/978-3-319-44899-2_15.
Mortoja, M. G., & Yigitcanlar, T. (2022). Factors influencing peri-urban growth: Empirical evidence from the Dhaka and Brisbane regions. *Remote Sensing Applications: Society and Environment, 26*, Article 100762. https://doi.org/10.1016/j.rsase.2022.100762
Nielsen, J. (2006). *The 90-9-1 rule for participation inequality in social media and N communities*. October 8. Nielsen Norman Group https://www.nngroup.com/articles/participation-inequality/.
Nieuwenhuijsen, M. J. (2020). Urban and transport planning pathways to carbon neutral, liveable and healthy cities; A review of the current evidence. *Environment International, 140*, Article 105661. https://doi.org/10.1016/j.envint.2020.105661
Nourmohammadi, Z., Lilasathapornkit, T., Ashfaq, M., Gu, Z., & Saberi, M. (2021). Mapping urban environmental performance with emerging data sources: A Case of urban greenery and traffic noise in Sydney, Australia. *Sustainability, 13*, 605. https://doi.org/10.3390/SU13020605, 2021Vol. 13, Page 605.
Barona, C. O., Labib, S. M., Chung, L., & Conway, T. M. (2023). Satisfaction with urban trees associates with tree canopy cover and tree visibility around the home. *npj Urban Sustainability, 3*(1). https://doi.org/10.1038/s42949-023-00119-8. Article 1.
O'Regan, A. C., Byrne, R., Hellebust, S., & Nyhan, M. M. (2022). Associations between Google Street View-derived urban greenspace metrics and air pollution measured using a distributed sensor network. *Sustainable Cities and Society, 87*, Article 104221. https://doi.org/10.1016/j.scs.2022.104221
Pietikainen, M., Nieminen, S., Marszalec, E., & Ojala, T. (1996). Accurate color discrimination with classification based on feature distributions. In *, 3. Proceedings of 13th international conference on pattern recognition* (pp. 833–838). https://doi.org/10.1109/ICPR.1996.547285. vol.3.
Rangel, J. C., Cruz, E., & Cazorla, M. (2022). Automatic understanding and mapping of regions in cities using Google Street View Images. *Applied Sciences, 12*(6). https://doi.org/10.3390/app12062971. Article 6.
Rathcke, B., & Lacey, E. P. (1985). Phenological patterns of terrestrial plants. *Annual Review of Ecology and Systematics, 16*(1), 179–214. https://doi.org/10.1146/annurev.es.16.110185.001143
Root, E. D., Silbernagel, K., & Litt, J. S. (2017). Unpacking healthy landscapes: Empirical assessment of neighborhood aesthetic ratings in an urban setting. *Landscape and Urban Planning, 168*, 38–47. https://doi.org/10.1016/j.landurbplan.2017.09.028
Rundle, A. G., Bader, M. D. M., & Mooney, S. J. (2022). Machine learning approaches for measuring neighborhood environments in epidemiologic studies. *Current Epidemiology Reports, 9*(3), 175–182. https://doi.org/10.1007/s40471-022-00296-7
Rzotkiewicz, A., Pearson, A. L., Dougherty, B. V., Shortridge, A., & Wilson, N. (2018). Systematic review of the use of Google Street View in health research: Major themes, strengths, weaknesses and possibilities for future research. *Health & Place, 52*, 240–246. https://doi.org/10.1016/j.healthplace.2018.07.001
Satellite Imaging Corporation. (2022). Sentinel-2A SatelliteSensor. https://www.satimagingcorp.com/satellite-sensors/other-satellite-sensors/sentinel-2a/; Last accessed: 1 November 2023.

Saw, L. E., Lim, F. K. S., & Carrasco, L. R. (2015). The Relationship between natural park usage and happiness does not hold in a tropical city-state. *PloS One, 10*(7), Article e0133781. https://doi.org/10.1371/journal.pone.0133781

Seiferling, I., Naik, N., Ratti, C., & Proulx, R. (2017). Green streets – Quantifying and mapping urban trees with street-level imagery and computer vision. *Landscape and Urban Planning, 165*, 93–101. https://doi.org/10.1016/j.landurbplan.2017.05.010

Shrestha, R., & Wynne, R. H. (2012). Estimating biophysical parameters of individual trees in an urban environment using small footprint discrete-return imaging lidar. *Remote Sensing, 4*(2). https://doi.org/10.3390/rs4020484. Article 2.

Song, J., Gasparrini, A., Fischer, T., Hu, K., & Lu, Y. (2023). Effect modifications of overhead-view and eye-level urban greenery on heat–mortality associations: Small-area analyses using case time series design and different greenery measurements. *Environmental Health Perspectives, 131*(9), Article 097007. https://doi.org/10.1289/EHP12589

Staves, C., Labib, S. M., Itova, I., Moeckel, R., Woodcock, J., & Zapata-Diomedi, B. (2023). Incorporating network-based built environmental attributes of walkability and cyclability into accessibility modelling: A pilot study for Greater Manchester. In *Proceedings of the 31st annual geographical information science research UK conference (GISRUK)*. https://doi.org/10.5281/zenodo.7825121

Stringam, B., Gerdes, J. H., & Anderson, C. K. (2023). Legal and ethical issues of collecting and using online hospitality data. *Cornell Hospitality Quarterly, 64*(1), 54–62. https://doi.org/10.1177/19389655211040434

Suppakittpaisarn, P., Lu, Y., Jiang, B., & Slavenas, M. (2022). How do computers see landscapes? Comparisons of eye-level greenery assessments between computer and human perceptions. *Landscape and Urban Planning, 227*, Article 104547. https://doi.org/10.1016/j.landurbplan.2022.104547

Tang, J., & Long, Y. (2019). Measuring visual quality of street space and its temporal variation: Methodology and its application in the Hutong area in Beijing. *Landscape and Urban Planning, 191*, Article 103436. https://doi.org/10.1016/j.landurbplan.2018.09.015

Torkko, J., Poom, A., Willberg, E., & Toivonen, T. (2023). How to best map greenery from a human perspective? Comparing computational measurements with human perception. *Frontiers in Sustainable Cities, 5*. https://www.frontiersin.org/articles/10.3389/frsc.2023.1160995.

Ulrich, R. S. (1984). View through a window may influence recovery from surgery. *Science, 224*(4647), 420–421. https://doi.org/10.1126/science.6143402

SciPy. (2022). SciPy documentation. https://docs.scipy.org/doc/scipy-1.9.0/; Last accessed: 1 November 2023.

Wang, R., Browning, M. H. E. M., Qin, X., He, J., Wu, W., Yao, Y., & Liu, Y. (2022). Visible green space predicts emotion: Evidence from social media and street view data. *Applied Geography, 148*, Article 102803. https://doi.org/10.1016/j.apgeog.2022.102803

Wang, R., Feng, Z., Pearce, J., Yao, Y., Li, X., & Liu, Y. (2021). The distribution of greenspace quantity and quality and their association with neighbourhood socioeconomic conditions in Guangzhou, China: A new approach using deep learning method and street view images. *Sustainable Cities and Society, 66*, Article 102664. https://doi.org/10.1016/j.scs.2020.102664

Wilkinson, M. D., Dumontier, M., Aalbersberg, I. J., Appleton, G., Axton, M., Baak, A., … Mons, B. (2016). The FAIR Guiding Principles for scientific data management and stewardship. *Scientific Data, 3*(1), 1–9.

Willberg, E., Poom, A., Helle, J., & Toivonen, T. (2023). Cyclists' exposure to air pollution, noise, and greenery: A population-level spatial analysis approach. *International Journal of Health Geographics, 22*(1), 5. https://doi.org/10.1186/s12942-023-00326-7

Wolf, K. L. (2005). Business district streetscapes, trees, and consumer response. *Journal of Forestry, 103*(8), 396–400. https://doi.org/10.1093/jof/103.8.396

Wong, N. H., Kwang Tan, A. Y., Tan, P. Y., Chiang, K., & Wong, N. C. (2010). Acoustics evaluation of vertical greenery systems for building walls. *Building and Environment, 45*(2), 411–420. https://doi.org/10.1016/j.buildenv.2009.06.017

United Nations, Department of Economic and Social Affairs, Population Division (2019). World Urbanization Prospects 2018: Highlights (ST/ESA/SER.A/421).

Wu, J., Cheng, L., Chu, S., Xia, N., & Li, M. (2020). A green view index for urban transportation: How much greenery do we view while moving around in cities? *International Journal of Sustainable Transportation, 14*(12), 972–989.

Xia, Y., Yabuki, N., & Fukuda, T. (2021). Development of a system for assessing the quality of urban street-level greenery using street view images and deep learning. *Urban Forestry & Urban Greening, 59*, Article 126995. https://doi.org/10.1016/j.ufug.2021.126995

Yang, J., Kang, Z., Cheng, S., Yang, Z., & Akwensi, P. H. (2020). An individual tree segmentation method based on watershed algorithm and three-dimensional spatial distribution analysis from airborne LiDAR point clouds. *IEEE Journal of Selected Topics in Applied Earth Observations and Remote Sensing, 13*, 1055–1067. https://doi.org/10.1109/JSTARS.2020.2979369

Yang, J., Zhao, L., Mcbride, J., & Gong, P. (2009). Can you see green? Assessing the visibility of urban forests in cities. *Landscape and Urban Planning, 91*(2), 97–104. https://doi.org/10.1016/j.landurbplan.2008.12.004

Yao, Y., Zhu, X., Xu, Y., Yang, H., Wu, X., Li, Y., & Zhang, Y. (2012). Assessing the visual quality of green landscaping in rural residential areas: The case of Changzhou, China. *Environmental Monitoring and Assessment, 184*(2), 951–967. https://doi.org/10.1007/s10661-011-2012-z

Yap, W., Chang, J.. H., & Biljecki, F. (2022). Incorporating networks in semantic understanding of streetscapes: Contextualising active mobility decisions. *Environment and Planning B: Urban Analytics and City Science*. https://doi.org/10.1177/23998083221138832, 23998083221138830.

Ye, Y., Richards, D., Lu, Y., Song, X., Zhuang, Y., Zeng, W., & Zhong, T. (2019). Measuring daily accessed street greenery: A human-scale approach for informing better urban planning practices. *Landscape and Urban Planning, 191*, Article 103434. https://doi.org/10.1016/j.landurbplan.2018.08.028

Yu, S., Yu, B., Song, W., Wu, B., Zhou, J., Huang, Y., & Mao, W. (2016). View-based greenery: A three-dimensional assessment of city buildings' green visibility using Floor Green View Index. *Landscape and Urban Planning, 152*, 13–26. https://doi.org/10.1016/j.landurbplan.2016.04.004

Yu, X., Zhao, G., Chang, C., Yuan, X., & Heng, F. (2019). BGVI: A new index to estimate street-side greenery using Baidu street view image. *Forests, 10*(1). https://doi.org/10.3390/f10010003. Article 1.

Zheng, X., & Amemiya, M. (2023). Method for applying crowd-sourced street-level imagery data to evaluate street-level greenness. *ISPRS International Journal of Geo-Information, 12*(3). https://doi.org/10.3390/ijgi12030108. Article 3.

Zijlema, W. L., Triguero-Mas, M., Cirach, M., Gidlow, C., Kruize, H., Grazuleviciene, R., & Litt, J. S. (2020). Understanding correlates of neighborhood aesthetic ratings: A European-based four city comparison. *Urban Forestry & Urban Greening, 47*, Article 126523. https://doi.org/10.1016/j.ufug.2019.126523